

# Thermoacoustic effects in supercritical fluids near the critical point: Resonance, piston effect, and acoustic emission and reflection

Akira Onuki

*Department of Physics Kyoto University, Kyoto 606-8502*

(Received 31 August 2007; published 26 December 2007)

We present a general theory of thermoacoustic phenomena in one phase states of one-component fluids. Singular behavior is predicted in supercritical fluids near the critical point. In a one-dimensional geometry we start with linearized hydrodynamic equations taking into account the effects of heat conduction in the boundary walls and the bulk viscosity. We introduce a coefficient  $Z(\omega)$  characterizing reflection of sound with frequency  $\omega$  at the boundary in a rigid cell. As applications, we examine acoustic eigenmodes, response to time-dependent perturbations, and sound emission and reflection. Resonance and rapid adiabatic changes are noteworthy. In these processes, the role of the thermal diffusion layers is enhanced near the critical point because of the strong critical divergence of the thermal expansion.

DOI: [10.1103/PhysRevE.76.061126](https://doi.org/10.1103/PhysRevE.76.061126)

PACS number(s): 64.60.-i, 05.70.Jk, 64.70.Fx, 62.60.+v

## I. INTRODUCTION

In highly compressible fluids, significant adiabatic changes can be achieved with propagation of sounds throughout the container at fixed volume [1]. Such adiabatic processes are ubiquitous, but are neglected in most hydrodynamic theories of compressible fluids. Among them, a well-known example is the piston effect near the gas-liquid critical point in a one-component fluid. It is caused by expansion or shrinkage of a thermal diffusion layer created when a boundary is heated or cooled. Sounds emitted from the layer then induce adiabatic changes in the interior. The density change in the layer is enhanced near the gas-liquid critical point because of the strong critical growth of the isobaric thermal expansion. As a result, macroscopic thermal equilibration times become much shorter at fixed volume (critical speeding up), despite the fact that the thermal diffusion constant  $D$  tends to zero at the criticality [2–11]. That is, if the boundary temperature is slightly changed, temperature homogenization occurs in the interior on a scale of the piston time [3]

$$t_1 = L^2/4(\gamma - 1)^2 D, \quad (1.1)$$

where  $L$  is the cell length and  $\gamma = C_p/C_V$  is the specific-heat ratio growing near the critical point. The time  $t_1$  is much shorter than the isobaric equilibration time  $L^2/4D$  for  $\gamma \gg 1$ . For example,  $t_1 = 6.3 \times 10^4 \epsilon^{1.65}$  s for  $\text{CO}_2$  at the critical density with  $L = 1$  cm. Hereafter,  $\epsilon = T/T_c - 1$  is the reduced temperature. The early experiments detected slow temperature and density changes in the interior on time scales much longer than the acoustic time  $L/c$ . The fast acoustic processes were examined by numerical simulations of the hydrodynamic equations of compressible fluids [6,12,13].

We may derive  $t_1$  in Eq. (1.1) using simple arguments. Let us apply a small heat  $\delta Q$  per unit area to a fluid from the boundary with area  $A$ . Then the volume of the thermal diffusion layers changes by  $(\partial \rho^{-1}/\partial s)_p A \delta Q(t)/T$ , where  $\rho$ ,  $s$ , and  $p$  are the mass density, the entropy per unit mass, and the pressure, respectively [see Eq. (2.48)]. This leads to the density change in the interior

$$\delta \rho = \frac{\rho}{T} \left( \frac{\partial T}{\partial p} \right)_s \frac{\delta Q}{L}, \quad (1.2)$$

where  $L = V/A$  is the cell length. The interior temperature deviation is caused adiabatically as

$$\delta T = (\gamma - 1) \delta Q / C_p L, \quad (1.3)$$

where  $C_p = \rho T (\partial s / \partial T)_p$  is the specific heat at constant pressure. In deriving these relations we have used the thermodynamic relations  $(\partial \rho^{-1} / \partial s)_p = (\partial T / \partial p)_s$  and  $\rho (\partial T / \partial p)_s (\partial T / \partial p)_s / T = (\gamma - 1) / C_p$  [see Eq. (2.9)]. If the boundary temperature is raised by  $T_1$  at  $t = 0$ , we have  $\delta Q \sim C_p \ell(t) T_1$  in the early stage, where  $\ell(t) = \sqrt{Dt}$  is the thickness of the thermal diffusion layer. The piston time (1.1) follows if we set  $\delta T = T_1/2$  at  $t = t_1$ .

We mention subsequent notable contributions related to the piston effect. Ferrell and Hao [14] found relevance of the heat conduction in the boundary walls in transient heat transport. That is, the thermal boundary condition of a cell containing a near-critical fluid crosses over from the isothermal to insulating one even for a metal boundary wall due to the critical divergence of the effusivity of the fluid [15]. The formula (1.1) should then be modified, because it is based on the isothermal boundary condition. More recently, Carlès and Dadzie [16,17] found that the bulk viscosity, which grows strongly near the critical point, can affect the hydrodynamics in the thermal diffusion layer. Gillis *et al.* [18] performed experiments of acoustic resonance in xenon, where the frequency and attenuation of the resonating modes were measured. For such long wavelength sounds, the heat conduction at the boundary is the dominant damping mechanism relatively far from the critical point, while the viscous effect in the bulk becomes more important closer to the critical point. They also presented thorough theoretical analysis of their data. The critical growth of the effusivity and the bulk viscosity of the fluid both serve to suppress the boundary damping, as confirmed experimentally and theoretically. Very recently, Miura *et al.* [19,20] measured acoustic density changes with precision of order  $10^{-7}$  g/cm<sup>3</sup> in near-critical  $\text{CO}_2$  on the acoustic time scale using an ultrasensitive inter-

ferometer. They detected emission and traversal of sound pulses with width of order  $5 \mu\text{s}$ , which were broadened as they moved through the cell and interacted with the boundary walls. Some of their data agreed with predictions, but most data remain unexplained. Afterwards, Carlès reproduced part of the measured density evolution relatively far from the critical point by analytically solving the linear hydrodynamic equations in the form of Laplace transforms and numerically inverting them [21].

In supercritical fluids, convection can easily be induced even by small thermal disturbances owing to the enhanced thermal expansion and a relatively small shear viscosity, as revealed by experiments [22–24] and by simulations [13,25–29]. As a unique aspect in Rayleigh-Bénard convection, overall temperature changes are induced by plume arrivals at the boundary walls due to the piston effect, leading to overshoot behavior observed in experiments of  $^3\text{He}$  near its critical point [22,26,27]. In turbulent convective states, significant noises of the adiabatic temperature changes were predicted [26], though not yet measured systematically. Recently, three-dimensional simulations of convection were performed in supercritical fluids [29]. Due to large thermal expansion near the critical point, jetlike fluid flow has been observed around a heated boundary [23,24]. In these processes, the plume motions governed by the shear viscosity are strongly influenced by large thermal expansion around a heater and by rapid adiabatic density and temperature changes achieved by sound propagation.

In this paper, we aim to present a general theory of thermoacoustic effects under realistic boundary conditions, including acoustic resonance to periodic perturbations, mechanical and thermal piston effects, and sound emission and reflection at a boundary. We experience these phenomena in our everyday life, but their understanding is still fragmentary even away from the critical point or even in the classical regime [30]. We will start with the linear hydrodynamics of supercritical fluids in a one-dimensional cell, neglecting side wall effects and convection for simplicity. The scope of this paper is hence limited. Particularly, we will clarify the influence of the decreasing effusivity ratio and the growing bulk viscosity in the thermal diffusion layers near the critical point, which was investigated by Gillis *et al.* in a complicated geometry [18].

The organization of this paper is as follows. In Sec. II, we will decompose fluid motions into sound modes and thermal diffusion modes with frequency  $\omega$ . These two modes are mixed at the boundary under each boundary condition. In Sec. III, we will study various thermoacoustic effects as applications. In the Appendix, the critical behavior of one-component fluids used in the text will be summarized.

## II. THEORETICAL BACKGROUND

Our linear theory can be used for one-component fluids in one phase states. Near the critical point, the hydrodynamic deviations are assumed to have spatial scales longer than the thermal correlation length  $\xi$ , but their typical frequency  $\omega$  can be higher than the relaxation rate of the critical fluctuations  $t_\xi^{-1}$ , where  $t_\xi \propto \epsilon^{-1.89}$  on the critical isochore [31]. For

such high frequencies  $\omega$ , the bulk viscosity  $\zeta$  behaves roughly as  $1/\omega$ , while  $\zeta \propto \epsilon^{-1.67}$  for  $\omega t_\xi < 1$  (see the Appendix) [32–34]. The critical singularity of the shear viscosity  $\eta$  is negligibly small, while the critical growth of the thermal conductivity  $\lambda$  arises from the convective motions of the critical fluctuations taking place on a short time scale of order  $\rho \xi^2 / \eta$  ( $\cong 2.8 \times 10^{-13} \epsilon^{-1.25}$  s for  $\text{CO}_2$ ). We assume  $\omega \ll \eta / \rho \xi^2$ , under which  $\lambda$  is independent of  $\omega$ .

### A. Linear hydrodynamics

The mass density, the temperature, the entropy (per unit mass), and the pressure are written as  $\rho$ ,  $T$ ,  $s$ , and  $p$ , respectively, with their small deviations being  $\delta\rho$ ,  $\delta T$ ,  $\delta s$ , and  $\delta p$ . The velocity in the  $x$  direction is written as  $v$ . These deviations depend on time  $t$  as  $\exp(i\omega t)$  and vary in space along the  $x$  axis. We may assume  $\omega > 0$  without loss of generality [see Eq. (3.1)]. These deviations may be regarded as the Fourier transformations of the space-time-dependent deviations with respect to time [ $= \int dt e^{-i\omega t}(\dots)$ ]. They obey the linear equations [30]

$$i\omega \delta\rho = -\rho v', \quad (2.1)$$

$$i\omega \rho v = -\delta p' + \rho \nu_\ell v'', \quad (2.2)$$

$$i\omega \rho T \delta s = \lambda \delta T''. \quad (2.3)$$

Here the prime denotes the differentiation with respect to  $x$ . We have two dissipative coefficients; one is the thermal conductivity  $\lambda$  and the other is

$$\nu_\ell = (\zeta + 4\eta/3)/\rho, \quad (2.4)$$

where  $\zeta$  and  $\eta$  are the bulk and shear viscosities, respectively. Using the thermodynamic derivatives we may express  $\delta s$  and  $\delta p$  in terms of  $\delta\rho$  and  $\delta T$  as

$$\rho T \delta s = C_V [\delta T - b_s^{-1} \delta\rho], \quad (2.5)$$

$$\delta p = \gamma^{-1} c^2 \delta\rho + (1 - \gamma^{-1}) a_s \delta T, \quad (2.6)$$

where  $c^2 = (\partial p / \partial \rho)_s$  is the square of the sound velocity,

$$\gamma = C_p / C_V \quad (2.7)$$

is the specific-heat ratio with  $C_p = \rho T (\partial s / \partial T)_p$  and  $C_V = \rho T (\partial s / \partial T)_\rho$  being the isobaric and constant-volume specific heat (per unit volume), respectively. To avoid cumbersome notation, we write

$$a_s = \left( \frac{\partial p}{\partial T} \right)_s, \quad b_s = \left( \frac{\partial \rho}{\partial T} \right)_s = c^{-2} a_s. \quad (2.8)$$

For low-frequency sounds, the adiabatic relations  $\delta p \cong a_s \delta T$  and  $\delta \rho \cong b_s \delta T$  should hold. We use the following thermodynamic identities [1]:

$$\left( \frac{\partial p}{\partial T} \right)_\rho = (1 - \gamma^{-1}) a_s = \rho c^2 C_V / T a_s. \quad (2.9)$$

The coefficients  $a_s = (\partial p / \partial T)_s$  and  $(\partial p / \partial T)_\rho$  both tend to the derivative  $(\partial p / \partial T)_{c_x}$  along the coexistence curve near the

critical point, where the corrections are of order  $\gamma^{-1}$  on the critical isochore [1].

Next we consider small hydrodynamic deviations by assuming the space dependence in the sinusoidal form  $\exp(iqx)$ . From Eqs. (2.3) and (2.5)  $\delta\rho$  and  $\delta T$  are related by

$$\delta T = \frac{i\omega c^2}{(i\omega + \gamma D q^2) a_s} \delta\rho, \quad (2.10)$$

where  $D = \lambda / C_p$  is the thermal diffusion constant. Equations (2.1)–(2.3) give the dispersion equation between  $q$  and  $\omega$ ,

$$[\omega^2 - (i\omega\nu_\ell + \gamma^{-1}c^2)q^2](i\omega + \gamma D q^2) = i\omega c^2(1 - \gamma^{-1})q^2. \quad (2.11)$$

If we set  $q = \omega/c\sqrt{X}$  or  $X = (\omega/cq)^2$ , the dimensionless quantity  $X$  obeys the quadratic equation,

$$X^2 - (1 + \Delta_v + \gamma\Delta_T)X + (1 + \gamma\Delta_v)\Delta_T = 0, \quad (2.12)$$

where we introduce two dimensionless coefficients representing the dissipation strength [18],

$$\Delta_v = i\omega\nu_\ell/c^2, \quad (2.13)$$

$$\Delta_T = i\omega D/c^2. \quad (2.14)$$

The ratio  $\Delta_v/\Delta_T = \nu_\ell/D$  grow strongly near the critical point (see the Appendix).

For given  $\omega$ , Eq. (2.11) or Eq. (2.12) yields four solutions  $q = \pm q_\pm = \pm\omega/c\sqrt{X_\pm}$ , where  $X_+$  and  $X_-$  are the solutions of Eq. (2.12) written as [18]

$$X_\pm = \frac{1}{2}(1 + \Delta_v + \gamma\Delta_T \mp \Xi) = \frac{2(1 + \gamma\Delta_v)\Delta_T}{1 + \Delta_v + \gamma\Delta_T \mp \Xi}, \quad (2.15)$$

where we define

$$\Xi = [(1 + \Delta_v - \gamma\Delta_T)^2 + 4(\gamma - 1)\Delta_T]^{1/2}, \quad (2.16)$$

with  $\text{Re } \Xi > 0$ . The second line of Eq. (2.15) follows from  $X_+X_- = (1 + \gamma\Delta_v)\Delta_T$ . The modes with  $q = \pm q_-$  represent the sound, while those with  $q = \pm q_+$  represent the thermal diffusion. We may define  $q_-$  and  $q_+$  such that  $\text{Re}(q_-/\omega) > 0$  and  $\text{Im } q_+ < 0$  hold. Hereafter  $\text{Re}(\dots)$  and  $\text{Im}(\dots)$  denote taking the real and imaginary part, respectively. It is convenient to introduce wave numbers  $k$  and  $\kappa$  by

$$k = q_- = \frac{\omega}{c\sqrt{X_-}}, \quad \kappa = iq_+ = \frac{i\omega}{c\sqrt{X_+}}. \quad (2.17)$$

The argument of  $X_-$  is in the range  $[0, \pi/2]$  for  $\omega > 0$ , leading to  $\text{Im } k < 0$ , which implies that sound waves propagating in the positive  $x$  direction ( $\propto e^{-ikx}$ ) are damped with increasing  $x$ .

As  $\omega \rightarrow 0$ , we may treat  $\Delta_v$  and  $\Delta_T$  as small quantities. To their first order we find  $X_+ \cong \Delta_T$  and  $X_- \cong 1 + \Delta_v + (\gamma - 1)\Delta_T$  so that  $\kappa \cong \sqrt{i\omega/D}$  and  $k \cong \omega/c - i\Gamma_s\omega^2/2c^3$ , where [30]

$$\Gamma_s = (\zeta + 4\eta/3)/\rho + (\gamma - 1)D \quad (2.18)$$

is the attenuation constant in the long wavelength limit. We have  $|\kappa| \gg |k|$  at low frequencies. For example,  $|k|$

$\sim 10^5 \text{ cm}^{-1}$  and  $|k| \sim 10^{-2} \text{ cm}^{-1}$  for  $\omega = 10^4 \text{ s}^{-1}$ ,  $D = 10^{-6} \text{ cm}^2 \text{ s}^{-1}$ , and  $c = 10^4 \text{ cm/s}$ . In a cell with length  $L$ , the strength of the bulk dissipation of sounds is represented by the damping factor  $\exp(-\delta_B L)$  with

$$\delta_B = -\text{Im } k \cong \Gamma_s \omega^2 / 2\rho c^3, \quad (2.19)$$

where the second line is the low-frequency expression. Mathematically, we may consider the high-frequency limit  $|\Delta_v| \gg 1$  and  $|\Delta_T| \gg 1$  neglecting the frequency dependence of the transport coefficients to derive the limiting behavior  $k \rightarrow (i\omega/\nu_\ell)^{1/2}$  and  $\kappa \rightarrow (i\omega/\gamma D)^{1/2}$ , though this limit is unrealistic. In this paper, we will assume  $|\Delta_T| \ll \gamma^{-1}$  in Eq. (2.34), because it is satisfied in realistic experimental conditions, as will be discussed.

## B. Solutions in a rigid cell

We consider small hydrodynamic perturbations behaving as  $e^{i\omega t}$  in a fluid in a rigid cell with length  $L$ . The density deviation can be expressed in the following linear combination:

$$\delta\rho = ae^{-\kappa x} + be^{\kappa(x-L)} + \alpha e^{ikx} + \beta e^{-ikx}. \quad (2.20)$$

The coefficients  $a$ ,  $b$ ,  $\alpha$ , and  $\beta$  depend on time as  $e^{i\omega t}$ . The first and second terms represent the deviations in the thermal diffusion layers. The thickness of the layers is given by  $1/|\kappa|$ , which is assumed to be much shorter than the cell length  $L$ , so

$$|\kappa| \gg 1/L. \quad (2.21)$$

In Eq. (2.20), the second (first) term is virtually zero near  $x=0$  ( $x=L$ ). The third term represents a sound propagating in the negative  $x$  direction, while the fourth term represents a sound propagating in the positive  $x$  direction. From Eq. (2.1) the velocity is expressed as

$$v = \frac{i\omega}{\rho\kappa} [ae^{-\kappa x} - be^{\kappa(x-L)}] - \frac{\omega}{\rho k} [\alpha e^{ikx} - \beta e^{-ikx}]. \quad (2.22)$$

If the boundary walls are rigid and fixed [35], we require  $v = 0$  at  $x=0$  and  $L$  to obtain

$$a = (\kappa/ik)(\alpha - \beta), \quad (2.23)$$

$$b = -(\kappa/ik)(\alpha e^{ikL} - \beta e^{-ikL}). \quad (2.24)$$

Note that the mass change in the thermal diffusion layers is  $(a+b)/\kappa$  and that in the interior is  $\alpha(e^{ikL}-1)/ik + \beta(1-e^{-ikL})/ik$  per unit area. From Eqs. (2.23) and (2.24) these two changes cancel, ensuring the overall mass conservation. Use of Eq. (2.10) gives the temperature deviation in the following linear combination:

$$\delta T = \frac{i\omega}{b_s} \left[ \frac{ae^{-\kappa x} + be^{\kappa(x-L)}}{i\omega - \gamma D \kappa^2} + \frac{\alpha e^{ikx} + \beta e^{-ikx}}{i\omega + \gamma D k^2} \right]. \quad (2.25)$$

Let  $\dot{Q}_0$  and  $\dot{Q}_L$  be the heat flux  $-\lambda \delta T'$  at  $x=0$  and  $L$ , respectively. Use of Eqs. (2.23)–(2.25) gives

$$\frac{\beta - \alpha}{\dot{Q}_0} = \frac{\beta - \alpha e^{2ikL}}{e^{ikL}\dot{Q}_L} = \frac{b_s(\gamma - 1)}{\lambda(1 + \gamma\Delta_v)} \frac{ik}{k^2 + \kappa^2}, \quad (2.26)$$

where  $b_s(\gamma - 1)/\lambda = \rho/Ta_s D$  with the aid of Eq. (2.9). The above quantities tend to the constant  $\rho/Ta_s c$  in the low-frequency limit. We may use Eq. (2.26) when  $\dot{Q}_0$  is a control parameter or when  $\dot{Q}_L$  is measurable.

The coefficients  $a$ ,  $b$ ,  $\alpha$ , and  $\beta$  can be determined if we specify the boundary conditions at  $x=0$  and  $L$ . Hereafter we assume no temperature discontinuity at the boundaries. In most theoretical calculations the boundary temperatures are fixed, but in some papers the bottom heat flux  $\dot{Q}_0$  is fixed [26]. In this paper, we consider a more realistic boundary condition of the temperature accounting for the thermal conduction in the boundary wall regions [14,18]. Here we assume that  $\delta T$  tends to zero in the solid far from the boundaries without heat input. In the solid region ( $x < 0$ ), the temperature deviation then decays as  $\delta T(0)e^{\kappa_w x}$  with

$$\kappa_w = (i\omega C_w / \lambda_w)^{1/2}, \quad (2.27)$$

where  $\lambda_w$  and  $C_w$  are the thermal conductivity and the heat capacity (per unit volume) of the solid, respectively. The  $1/|\kappa_w|$  is the thickness of the thermal diffusion layer in the solid and is assumed to be shorter than the thickness of the wall. Without temperature discontinuity at the boundary, the energy balance at  $x=0$  yields

$$\delta T' = \lambda_w \kappa_w \delta T / \lambda = a_w (i\omega / D)^{1/2} \delta T, \quad (2.28)$$

where  $\delta T$  and  $\delta T'$  are the values at  $x=0$ . In the second line, the coefficient  $a_w$  is the effusivity ratio [15,18],

$$a_w = (C_w \lambda_w / C_p \lambda)^{1/2}. \quad (2.29)$$

For CO<sub>2</sub> in a Cu cell [20] we have  $a_w = 3 \times 10^3 \epsilon^{0.92}$ . The boundary temperature at  $x=0$  is fixed or  $\delta T(0)=0$  for  $a_w \rightarrow \infty$ , while the boundary is thermally insulating or  $(d\delta T/dx)_{x=0}=0$  as  $a_w \rightarrow 0$ . On the other hand, if the other boundary wall in the region  $x > L$  is made of the same material, the boundary condition at  $x=L$  reads

$$\delta T' = -a_w (i\omega / D)^{1/2} \delta T, \quad (2.30)$$

with the same  $a_w$  as in Eq. (2.28), where  $\delta T$  and  $\delta T'$  are the values at  $x=L$ .

The boundary conditions at  $x=0$  give Eqs. (2.23) and (2.28), from which we may readily calculate the reflection factor  $Z \equiv \beta/\alpha$  between the outgoing and incoming sound waves. It is convenient to introduce the combination,

$$W = \frac{\alpha - \beta}{\alpha + \beta} = \frac{1 - Z}{1 + Z}, \quad (2.31)$$

because  $W$  is a small quantity in our system. Some calculations yield a general expression,

$$W = \frac{-ik(i\omega - \gamma D \kappa^2) / \kappa}{i\omega + \gamma D k^2 + \sqrt{i\omega D (\kappa^2 + k^2)} / a_w \kappa}, \quad (2.32)$$

in terms of  $k$  and  $\kappa$ . In the case of a thermally insulating boundary, we have  $W=0$  and  $Z=1$  by setting  $a_w \rightarrow 0$  in Eq. (2.32). The interaction of sounds and the boundary wall is

characterized by  $Z$  or  $W$ , where the wall properties appear only through the effusivity ratio  $a_w$  and the system length  $L$  does not appear.

### C. Adiabatic condition in the interior

We will clarify an upper bound of the frequency, below which the sound motions in the interior are *adiabatic* or without entropy deviations. Under this adiabatic condition, the results from the linear hydrodynamic equations can be much simplified, so it is crucial in the following calculations.

Far from the boundary walls or outside the thermal diffusion layers, we may neglect the localized modes to obtain the interior hydrodynamic deviations. From Eqs. (2.5), (2.6), and (2.25), those of the density, temperature, and pressure are related by

$$\begin{aligned} \delta \rho &= [1 + \gamma D k^2 / i\omega] b_s \delta T, \\ \delta p &= [1 + D k^2 / i\omega] a_s \delta T. \end{aligned} \quad (2.33)$$

Here  $x$  and  $L-x$  are much longer than  $1/|\kappa|$ . The second terms in the brackets arise from a small entropy deviation in the interior. Since  $\gamma > 1$ , the usual adiabatic relations hold in the interior under the condition

$$|\gamma D k^2 / i\omega| \sim \gamma |\Delta_T| \ll 1 \quad \text{or} \quad \omega \ll c^2 / \gamma D, \quad (2.34)$$

where  $\Delta_T$  is defined by Eq. (2.14). This condition is well satisfied in the usual hydrodynamic processes. Even near the critical point, the time  $t_{ad} \equiv \gamma D / c^2$  remains very short. For example,  $t_{ad} = 7.6 \times 10^{-14} \epsilon^{-0.62}$  s for CO<sub>2</sub>.

Under Eq. (2.34) we have  $\Xi \cong 1 + \Delta_v$  so that  $X_+$  and  $X_-$  in Eq. (2.15) are approximated as

$$X_+ = \frac{1 + \gamma \Delta_v}{1 + \Delta_v} \Delta_T, \quad X_- = 1 + \Delta_v. \quad (2.35)$$

The wave numbers  $k$  and  $\kappa$  are expressed as

$$\kappa = \left( \frac{i\omega}{D} \right)^{1/2} \left( \frac{1 + \Delta_v}{1 + \gamma \Delta_v} \right)^{1/2}, \quad k = \frac{\omega/c}{\sqrt{1 + \Delta_v}}. \quad (2.36)$$

We retain  $\Delta_v$ , since it becomes appreciable near the critical point because of the strong critical divergence of  $\zeta$ . As will be discussed in the Appendix,  $\zeta \cong \rho c^2 R_B t_\xi$  for  $\omega t_\xi < 1$ , where  $R_B \cong 0.03$  is a universal number and  $t_\xi = \xi^2 / D$  is the characteristic time of the critical fluctuations with  $\xi$  being the correlation length. Carlès found the dependence of  $\kappa$  on the singular combination  $\gamma \zeta$  as in Eq. (2.36) [16,17]. By setting  $\gamma \Delta_v = i\omega t_B$ , we introduce a new characteristic time  $t_B$  as

$$t_B = \gamma \zeta / \rho c^2 = R_B \gamma t_\xi. \quad (2.37)$$

Then  $t_B \gg t_\xi$  once  $R_B \gamma \gg 1$ . For CO<sub>2</sub>,  $t_B = 1.9 \times 10^{-15} \epsilon^{-3.0}$  s. See Table 1 and Fig. 1 for the characteristic times with  $L = 1$  cm, where  $t_B$  exceeds the acoustic time  $L/c$  for  $\epsilon < 3 \times 10^{-4}$  and the modified piston time  $t_1'$  [to be introduced in Eq. (3.16)] for  $\epsilon < 3 \times 10^{-5}$ . There can be a sizable frequency range with  $t_B^{-1} < \omega < t_\xi^{-1}$  at small  $\epsilon$ , where  $\kappa$  becomes independent of  $\omega$  as

TABLE I. Parameters of CO<sub>2</sub> in a Cu cell with  $L=1$  cm for  $\epsilon=10^{-3}$  (first line),  $10^{-4}$  (second line), and  $10^{-5}$  (third line). Times are in seconds.

$\gamma$	$a_w$	$t_\xi \times 10^6$	$t_B \times 10^6$	$L/c \times 10^4$	$t'_1$	$t_2 \times 10^8$
260	5.0	0.24	1.9	0.71	1.0	0.12
3600	0.63	18	1900	0.83	0.1	1.7
$5 \times 10^4$	0.075	1300	$1.7 \times 10^6$	0.98	0.08	3.0

$$\kappa \equiv (\rho c^2 / \gamma D \zeta)^{1/2} \cong (R_B \gamma)^{-1/2} \xi^{-1}. \quad (2.38)$$

The thickness of the thermal diffusion layer  $1/|\kappa|$  remains longer than  $\xi$  by  $(R_B \gamma)^{1/2}$ . Also from the expression of  $k$  in Eq. (2.36) we write the sound dispersion relation as  $k = \omega / c^*(\omega)$ , where we define the complex sound velocity [1],

$$c^*(\omega) = c \sqrt{1 + \Delta_v}, \quad (2.39)$$

whose critical behavior will be discussed in the Appendix.

As  $\epsilon$  is decreased, we first encounter the regime where  $W$  grows but  $a_w \gg 1$  and  $\omega t_B \ll 1$  still hold. However, the critical growth of  $W$  is eventually suppressed by the growing  $a_w^{-1}$  and  $\zeta$ . If we use Eqs. (2.35) and (2.36) under Eq. (2.34), we approximate  $W$  in Eq. (2.32) as

$$W = \frac{(\gamma - 1) \sqrt{\Delta_T}}{(1 + \Delta_v) X_v}, \quad (2.40)$$

where we define

$$X_v = \sqrt{1 + \gamma \Delta_v} + a_w^{-1} \sqrt{1 + \Delta_v}. \quad (2.41)$$

Here  $X_v \cong 1 + a_w^{-1}$  for  $\omega t_B \ll 1$  and  $X_v \cong (i \omega t_B)^{1/2} + a_w^{-1}$  for  $\omega t_B \gg 1$ . Thus  $X_v \cong (i \omega t_B)^{1/2}$  holds for  $\omega t'_B \gg 1$ , where it is convenient to define

$$t'_B = t_B (1 + a_w^{-1})^{-2}, \quad (2.42)$$

since  $t'_B \cong t_B$  for  $a_w \gg 1$  and  $t'_B \cong t_B a_w^2$  for  $a_w \ll 1$ .

For  $\omega \ll t_B^{-1}$ , the viscous effect is negligible, leading to the classical expression,

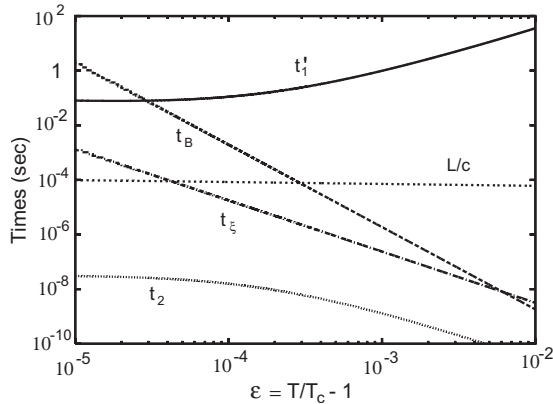


FIG. 1. Characteristic times  $t_\xi$  in Eq. (A4),  $t_B$  in Eq. (2.37),  $t_2$  in Eq. (2.43),  $t'_1$  in Eq. (3.16), and  $L/c$  vs  $\epsilon = T/T_c - 1$  for CO<sub>2</sub> in a Cu cell with  $L=1$  cm.

$$W = (\gamma - 1) \sqrt{\Delta_T} / (1 + a_w^{-1}) = \sqrt{it_2 \omega}, \quad (2.43)$$

which is valid not very close to the critical point. We may introduce a characteristic time  $t_2$  defined by

$$t_2 = (1 + a_w^{-1})^{-2} (\gamma - 1)^2 D / c^2, \quad (2.44)$$

which includes the effect of the heat conduction in the wall. The time  $t_2$  will appear in the formulas for reflection in Sec. III E. As shown in Table I and Fig. 1,  $t_2$  is very short even compared with  $t_\xi$ . In the literature (see Sec. 77 of Ref. [30]), it is argued that the amplitude of a plane wave sound is decreased by the factor  $(\gamma - 1) \sqrt{2D\omega} / c$  upon reflection at an isothermal boundary wall. This factor is obviously equal to  $1 - |Z| \cong 2 \operatorname{Re} W$  from Eq. (2.43).

In Fig. 2,  $\operatorname{Re} W$  and  $\operatorname{Im} W$  are displayed as functions of  $\omega$  at  $\epsilon = 10^{-3}$  and  $10^{-4}$ . While  $\omega t_B < 1$ , they increase with increasing  $\omega$  obeying Eq. (2.43). After  $\omega$  exceeds  $t_B^{-1}$ ,  $\sqrt{1 + \gamma \Delta_v}$  becomes  $\sqrt{\gamma \Delta_v}$  in Eq. (2.41); then,  $\operatorname{Re} W$  tends to saturate and  $\operatorname{Im} W$  decreases. In fact, for  $\omega t'_B \gg 1$ , we have  $X_v \cong \sqrt{\gamma \Delta_v}$  and

$$W \cong (\gamma D / \nu_\ell)^{1/2} \cong W_0 \epsilon^{0.64}, \quad (2.45)$$

where  $W_0 \cong 2.1$  for CO<sub>2</sub>. Also as a function of  $\epsilon$ ,  $\operatorname{Re} W$  exhibits a maximum around the reduced temperature at which  $t_B \sim \omega^{-1}$ , as will be shown in Fig. 3. Growing  $a_w^{-1} (\propto \epsilon^{-1.14})$  further serves to decrease  $W$ . Thus, even close to the critical point, we find  $|W| \ll 1$  and

$$Z = 1 - 2W + \dots \quad (2.46)$$

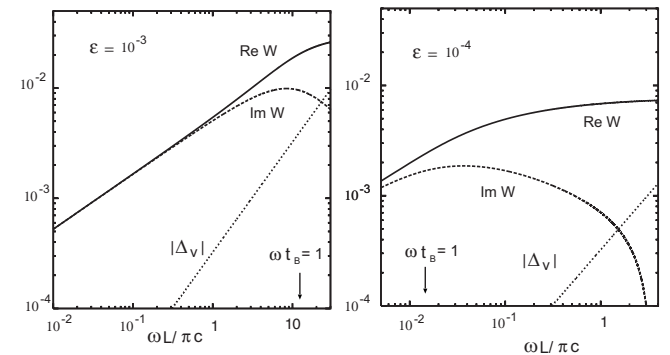


FIG. 2.  $\operatorname{Re} W$ ,  $\operatorname{Im} W$ , and  $|\Delta_v| = \omega \zeta / \rho c^2$  vs  $\omega L / \pi c$  at  $\epsilon = 10^{-3}$  (left) and  $10^{-4}$  (right) for CO<sub>2</sub> in a Cu cell with  $L=1$  cm. As  $\omega$  exceeds  $t_B^{-1}$ ,  $\operatorname{Re} W$  tends to saturate and  $\operatorname{Im} W$  decreases, due to the growing bulk viscosity and the decreasing effusivity ratio.

### D. Hydrodynamic variables in the adiabatic condition

Under Eq. (2.34) we obtain simple expressions for the deviations of the temperature, the pressure, and the entropy including  $\Delta_v$ . From Eqs. (2.5), (2.6), (2.9), and (2.20) we find

$$\delta T = \left( \frac{\delta T}{\partial \rho} \right)_p (1 + \gamma \Delta_v) [\delta \rho]_b + b_s^{-1} [\delta \rho]_{in}, \quad (2.47)$$

$$\delta s = \left( \frac{\delta s}{\partial \rho} \right)_p (1 + \Delta_v) [\delta \rho]_b, \quad (2.48)$$

$$\delta p = -c^2 \Delta_v [\delta \rho]_b + c^2 [\delta \rho]_{in}, \quad (2.49)$$

where  $[\delta \rho]_b = a e^{-\kappa x} + b e^{\kappa(x-L)}$  is the density deviation localized near the boundaries and  $[\delta \rho]_{in} = \alpha e^{ikx} + \beta e^{-ikx}$  is the interior density deviation. In deriving Eq. (2.47) use has been made of the thermodynamic relation  $(1 - \gamma) b_s = (\partial \rho / \partial T)_p$ . Under Eq. (2.34), the entropy deviation  $\delta s$  is localized near the boundaries, while the localized part of the pressure deviation  $\delta p$  is nonvanishing to satisfy  $i\omega \rho v = -\delta p' + \rho v_\ell v'' = -\delta p' - i\omega v_\ell \delta p' \rightarrow 0$  as  $x \rightarrow 0$  and  $L$  in Eq. (2.2). Note that the  $xx$  component of the stress tensor is given by  $\Pi_{xx} = p - \rho v_\ell v'$  and its deviation contains no localized part and behaves as

$$\delta \Pi_{xx} = c^*(\omega)^2 [\delta \rho]_{in}, \quad (2.50)$$

where  $c^*(\omega)$  is defined by Eq. (2.39). Equations (2.48) and (2.50) are natural consequences in the adiabatic condition, readily yielding nontrivial Eqs. (2.47) and (2.49) from Eqs. (2.5) and (2.6).

We examine the temperature and pressure deviations close to the boundary at  $x=0$  by assuming Eqs. (2.23) and (2.28) and setting  $\beta = Z\alpha$  as an example. In this case the density ratio  $[\delta \rho]_b / [\delta \rho]_{in}$  tends to  $(\gamma - 1) / X_v \sqrt{1 + \gamma \Delta_v}$  as  $x \rightarrow 0$ , so that

$$b_s \delta T = (\alpha + \beta) \left[ 1 - \frac{1}{X_v} \sqrt{1 + \gamma \Delta_v} e^{-\kappa x} \right], \quad (2.51)$$

$$\frac{\delta p}{c^2} = (\alpha + \beta) \left[ 1 - \frac{(\gamma - 1) \Delta_v}{X_v \sqrt{1 + \gamma \Delta_v}} e^{-\kappa x} \right], \quad (2.52)$$

where  $0 < x \ll 1/|k|$ . The velocity behaves as  $v = (\omega / \rho k) (\beta - \alpha) (1 - e^{-\kappa x})$  from Eq. (2.23). From Eqs. (2.51) and (2.52) we draw the following. (i) For the insulating case  $a_w \rightarrow 0$ , the coefficients of  $e^{-\kappa x}$  in the brackets in Eqs. (2.51) and (2.52) vanish. (ii) For the isothermal case  $a_w \rightarrow \infty$ , that in Eq. (2.51) tends to unity, leading to  $\delta T \rightarrow 0$  at  $x=0$ , and that in Eq. (2.52) tends to  $(\gamma - 1) \Delta_v / (1 + \gamma \Delta_v)$ . (iii) Generally, for  $\omega t'_B \gg 1$ , they both tend to unity and the hydrodynamic variations in the thermal diffusion layer are diminished, where  $t'_B$  is defined by Eq. (2.42). (iv) In the original work [3], the pressure homogeneity throughout the interior and the thermal diffusion layers was assumed, while the density deviations in the two regions are very different. We recognize that the pressure homogeneity holds only in the low-frequency limit  $\omega t'_B \ll 1$ .

## III. APPLICATIONS

### A. Acoustic modes in a cell

Gillis *et al.* [18] calculated the acoustic eigenmodes for their experimental geometry, taking into account the growing  $a_w^{-1}$  and  $\zeta$ . In the following, we will present a simpler version in the one-dimensional cell,  $0 < x < L$ , taking into account these two ingredients. In this case  $\omega$  is treated as one of the eigenvalues and is complex, while we have assumed  $\omega > 0$  in the previous section. Then  $\omega$  should have a positive imaginary part for the stability of the system. Here  $\sqrt{i\omega} = (1+i)\sqrt{|\omega|/2}$  for  $\omega > 0$ , while  $\sqrt{i\omega} = (1-i)\sqrt{|\omega|/2}$  for  $\omega < 0$ . The latter follows from the requirement that the real part of  $\kappa$  in Eq. (2.17) should be positive. For general complex  $\omega$ , all the quantities introduced so far should be functions of  $\omega$  analytic for  $\text{Re}(i\omega) > 0$  or for  $\text{Im} \omega < 0$ . Therefore,  $X_\pm(-\omega) = X_\pm(\omega^*)^*$  and

$$Z(-\omega^*) = Z(\omega)^*, \quad W(-\omega^*) = W(\omega)^*, \quad (3.1)$$

where  $\omega^*$  is the complex conjugate of  $\omega$ .

Under the boundary conditions (2.28) and (2.30), the interior density deviation is expressed as

$$\delta \rho = \alpha (e^{ikx} + Z e^{-ikx}) = \alpha' (e^{ik(L-x)} + Z e^{-ik(L-x)}), \quad (3.2)$$

in terms of  $Z = \beta / \alpha$ . The first and second lines follow from Eqs. (2.28) and (2.30), respectively, and should coincide so that  $\alpha' e^{ikL} = \beta$  and  $\alpha' Z e^{-ikL} = \alpha$ , leading to  $Z e^{-ikL} = Z^{-1} e^{ikL}$ . We now find the condition of the eigenmodes,

$$Z = \pm e^{ikL}, \quad (3.3)$$

where  $+$  corresponds to even modes and  $-$  to odd modes. Namely, the density and temperature deviations are even (odd) functions of  $x - L/2$  for the even (odd) modes. For  $W = (1 - Z) / (1 + Z)$  calculated in Eq. (2.32) or Eq. (2.40), we obtain

$$\begin{aligned} W &= -i \tan(kL/2) \quad (\text{even modes}) \\ &= i \cot(kL/2) \quad (\text{odd modes}). \end{aligned} \quad (3.4)$$

Since  $W$  is small as in Fig. 2, the eigenfrequencies  $\omega_n$  ( $n = 1, 2, 3, \dots$ ) are nearly equal to  $n\pi c^* / L$ , where  $c^*$  is defined by Eq. (2.39). The leading correction from  $W$  can be written as

$$\begin{aligned} \omega_n &= (n\pi + 2iW + \dots) c^* / L \\ &= [1 + i\alpha_\lambda + i\alpha_\zeta + \dots] \text{Re } \omega_n, \end{aligned} \quad (3.5)$$

where  $n=2, 4, \dots$  for the even modes and  $n=1, 3, \dots$  for the odd modes. We assume small bulk damping  $|\Delta_v| \ll 1$  and define

$$\alpha_\lambda = \frac{2}{n\pi} \text{Re } W, \quad \alpha_\zeta = \frac{n\pi \text{Im } c^*}{L \text{Re } \omega_n}, \quad (3.6)$$

where  $\alpha_\lambda$  represents the boundary damping and  $\alpha_\zeta$  the bulk damping. For  $\omega t'_\xi < 1$  we may set  $\alpha_\zeta = n\pi \zeta / 2\rho cL$ . The resonance quality factor  $Q^{-1}$  [18] is equal to  $2(\alpha_\lambda + \alpha_\zeta)$  in our notation. The resonance frequency including the shift is given by the real part,

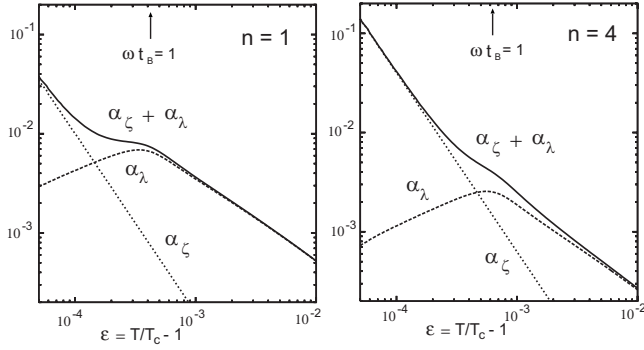


FIG. 3. Normalized damping constants  $\alpha_\lambda$ ,  $\alpha_\zeta$ , and  $\alpha_\lambda + \alpha_\zeta$  defined by Eqs. (3.5) and (3.6) vs  $\epsilon = T/T_c - 1$  for  $n=1$  (left) and  $n=4$  (right). The resonant frequencies are close to  $\omega = n\pi c/L \sim n \times 4 \times 10^4 \text{ s}^{-1}$ , which are exceeded by  $t_B^{-1}$  close to the critical point as marked by the arrows.

$$\text{Re } \omega_n = (n\pi - 2 \text{Im } W + \dots) \text{Re } c^*/L. \quad (3.7)$$

The frequency  $\omega$  in  $c^*$  and  $W$  may be equated with  $\text{Re } \omega_n$ .

In Fig. 3, we show  $\alpha_\lambda$ ,  $\alpha_\zeta (= n\pi\zeta/2\rho cL)$ , and the sum  $\alpha_\lambda + \alpha_\zeta$  as functions of  $\epsilon$  in the regime  $\omega t_\xi < 1$  for the odd mode of  $n=1$  and the even mode of  $n=4$  for  $\text{CO}_2$  in a Cu cell with  $L=1 \text{ cm}$ . We notice the following. (i) For such long wavelength sounds, the boundary damping is relevant far from the critical point, but the bulk damping eventually dominates close to the critical point. (ii) In accord with the discussion around Eq. (2.45),  $\alpha_\lambda$  decreases on approaching the criticality in the region of  $t_B > \omega^{-1} \sim L/n\pi c$ , with a maximum at  $\omega t_B \sim 1$ . As a result, the curve of the sum  $\alpha_\lambda + \alpha_\zeta$  is flattened considerably around  $t_B \sim \omega^{-1}$ .

These theoretical results are consistent with the experimental data by Gillis *et al.* [18]. They performed the resonance experiment over a wide range of  $\omega t_\xi$  (up to about 200) to measure the frequency-dependent bulk viscosity. In agreement with the theory [1,3],  $\alpha_\zeta$  or  $\omega\zeta/\rho c^2$  became independent of  $\epsilon$  in the high-frequency regime  $\omega t_\xi > 1$  [see Eq. (A6) in the Appendix].

### B. Periodic perturbations

Periodic perturbations may be applied to a fluid in a cell in various manners. Resonance can occur when the frequency  $\omega$  is close to  $\text{Re } \omega_n$ . It is sharp for small  $\text{Im } \omega_n$ . We will give three boundary conditions at  $x=0$  leading to resonance. We assume the boundary condition Eq. (2.30) at  $x=L$ . Then use of Eq. (3.2) yields  $\alpha = \beta Z e^{-2ikL}$ . The interior density deviation is of the form

$$\delta\rho = \beta e^{-ikx} + \beta Z e^{ikx-2ikL}, \quad (3.8)$$

where the second term arises from the reflection at  $x=L$ .

The bulk damping of the reflected waves is represented by  $|e^{-ikL}| = e^{-\delta_B L}$ . From Eq. (2.19)  $\delta_B$  is expressed as

$$\delta_B \cong A_B (\omega/\pi c)^2, \quad (3.9)$$

in the low-frequency regime  $\omega t_\xi < 1$ . We find  $A_B = 0.5 \times 10^{-3} \text{ cm}$  and  $0.03 \text{ cm}$  at  $\epsilon = 10^{-3}$  and  $10^{-4}$ , respectively, for

$\text{CO}_2$ . In the relatively high-frequency range  $\omega > (2A_B)^{-1/2} \pi c/L$ , the factor  $e^{-2ikL} (\propto e^{-2\delta_B L})$  becomes negligibly small. Then, near the boundary,  $\delta\rho$  consists of the outgoing wave only, resulting in no resonance. On the other hand, in the high-frequency regime  $\omega t_\xi > 1$ , Eq. (A7) gives

$$\delta_B \cong \omega \text{Im } c^*/(\text{Re } c^*)^2 \cong 0.13\omega/\pi \text{Re } c^*. \quad (3.10)$$

This means that a sound emitted at  $x=0$  reaches the other end with the damping factor  $e^{-0.13}$  for the first resonance frequency  $\omega \cong \pi \text{Re } c^*/L$ .

### 1. Temperature oscillation

Zhong *et al.* [11] measured a density change induced by boundary temperature oscillation in near-critical  $^3\text{He}$ , where the frequency was very low ( $\omega/2\pi < 2 \text{ Hz}$ ) and the bulk viscosity was not important. However, they could measure in-phase and out-of-phase response in agreement with the original theory [3]. Here we consider temperature oscillation at higher frequencies.

In the first example, the temperature in the wall region  $x < 0$  is oscillated, while the boundary walls are mechanically fixed. More precisely, we require  $\delta T \rightarrow T_w \propto e^{i\omega t}$  as  $x \rightarrow -\infty$ ; then,  $\delta T(x) = e^{\kappa_w x} [\delta T(0) - T_w] + T_w$  in the region  $x < 0$ . Here  $T_w$  is an externally applied parameter. The thermal boundary condition at  $x=0$  is then given by

$$\delta T' = a_w (i\omega/D)^{1/2} (\delta T - T_w), \quad (3.11)$$

as a generalization of Eq. (2.28). Some calculations using Eqs. (2.23) and (2.25) give the response function defined by  $R_T \equiv \beta/b_s T_w$  in the form

$$R_T = \frac{1}{2} (1 + \gamma D k^2 / i\omega) \frac{1 - Z}{1 - Z^2 e^{-2ikL}}. \quad (3.12)$$

Notice that  $R_T$  diverges as  $R_T \cong cW/2iL(\omega - \omega_n)$  for  $\omega \cong \omega_n$  ( $n=1, 2, \dots$ ) in the complex  $\omega$  plane from Eq. (3.3). Under the adiabatic condition (2.34), the interior temperature deviation is expressed as

$$\delta T = b_s^{-1} \delta\rho = (e^{-ikx} + Z e^{ikx-2ikL}) R_T T_w. \quad (3.13)$$

Furthermore, neglecting  $\gamma D k^2 / i\omega$  in Eq. (3.12) and using  $|W| \ll 1$  (see Fig. 2), we obtain

$$R_T \cong W/[1 - (1 - 4W)e^{-2ikL}]. \quad (3.14)$$

In Fig. 4, we plot the absolute value  $|R_T|$  calculated from Eq. (3.12) vs the normalized frequency  $\omega L/\pi c$  at  $\epsilon = 10^{-3}$  and  $10^{-4}$ , using the data for  $\text{CO}_2$  in a Cu cell with  $L=1 \text{ cm}$  [20]. It exhibits peaks at  $\omega \cong n\pi c/L$  as expected, but its peak heights do not exceed  $1/2$  due to the small factor  $1-Z \cong 2W$  in the numerator in Eq. (3.12). As discussed below Eq. (3.9), the resonant peaks should disappear for  $\omega L/\pi c > (2A_B)^{-1/2}$ , where we may neglect  $e^{-2ikL}$  in  $R_T$  to obtain  $R_T \cong W$ . These results are in accord with Fig. 4, since  $(2A_B)^{-1/2} \cong 30$  and  $4$  for  $\epsilon = 10^{-3}$  and  $10^{-4}$ , respectively.

In the low-frequency case  $\omega \ll c/L$ , the interior deviations become nearly homogeneous. Figure 1 indicates that  $t_B$  can much exceed  $L/c$  very close to the critical point, while  $|\Delta_v| \ll 1$  holds. Thus, retaining  $\gamma\Delta_v$ , we set  $e^{ikL} \cong 1 + ikL$  and

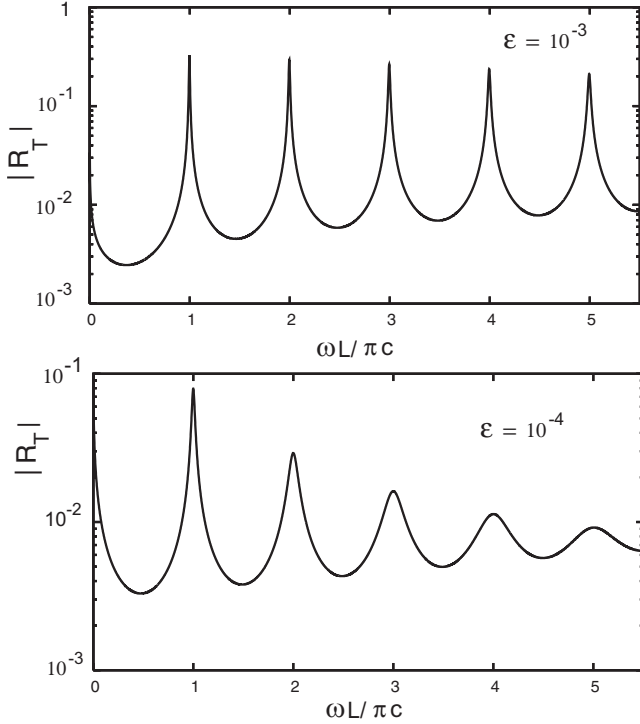


FIG. 4. Absolute value of the response function  $R_T(\omega)$  in Eq. (3.12) vs  $\omega L/\pi c$  on a semilogarithmic scale for  $\epsilon=10^{-3}$  (upper panel) and  $10^{-4}$  (lower panel) applicable for  $\text{CO}_2$  in a Cu cell with  $L=1$  cm.

$1+\Delta_v \cong 1$  and use Eqs. (2.40) and (3.12) to find

$$R_T \cong \frac{1}{4} [\sqrt{i\omega t_1} X_v + 1]^{-1}, \quad (3.15)$$

where  $t_1$  is defined by Eq. (1.1) and  $X_v$  by Eq. (2.41). If  $\omega \ll t_B^{-1}$ , we further have  $R_T \cong (\sqrt{i\omega t_1} + 1)^{-1}/4$  with

$$t_1' = (1 + a_w^{-1})^2 t_1 = (1 + a_w^{-1})^2 L^2/4(\gamma - 1)^2 D, \quad (3.16)$$

which is related to  $t_2$  in Eq. (2.44) by  $t_1' t_2 = L^2/4c^2$ . The  $t_1'$  first decreases as  $t_1 \sim \epsilon^{2.26}$  for  $a_w \gg 1$  but finally weakly increases as  $t_1 a_w^2 \cong \epsilon^{-0.22}$  for  $a_w \ll 1$ . See Fig. 1 for the curve of  $t_1'$ . As will be discussed in Sec. III C,  $t_1'$  is the piston time including the effect of the wall heat conduction [14].

We need to know when  $|\sqrt{i\omega t_1} X_v| \gg 1$  is realized. For  $a_w \gg 1$  it holds for  $\omega \gg 1/t_1$ . For  $a_w \ll 1$  we have  $\sqrt{\omega t_1} X_v \cong a_w \sqrt{1 + it_B/t_1} + 1$  at  $\omega = 1/t_1$ . Thus, for any  $a_w$ , the condition of  $|\sqrt{i\omega t_1} X_v| \gg 1$  is simply given by  $\omega t_1' \gg 1$  under the condition

$$t_B'/t_1' = (1 + a_w^{-1})^{-4} t_B/t_1 \ll 1, \quad (3.17)$$

where  $t_B'$  is defined by Eq. (2.42). For  $a_w < 1$ , the above condition becomes  $a_w^4 t_B/t_1 = A_v \epsilon^{-0.97}/L^2 \ll 1$ . For  $\text{CO}_2$  in a Cu cell, we find  $A_v = 2 \times 10^{-6}$  with  $L$  in cm, so this condition is well satisfied for  $\epsilon \gg 2 \times 10^{-6}$  with  $L=1$  cm. This crossover reduced temperature depends on  $L$  roughly as  $L^{-2}$ . On the other hand, if  $\omega t_1' \ll 1$  under Eq. (3.17), we find

$$\delta T \cong T_w/2, \quad (3.18)$$

in the interior. Note that the reverse condition of Eq. (3.17),  $a_w^4 t_B/t_1 > 1$ , holds extremely close to the critical point, where  $|\sqrt{i\omega t_1} X_v| > 1$  and  $R_T \cong 1/4i\omega \sqrt{t_1 t_B}$  are obtained for  $\omega \gg (t_1 t_B)^{-1/2}$ . See the discussion below Eq. (3.32) for the relaxation behavior in this ultimate regime.

## 2. Mechanical oscillation

In the second example, the boundary wall at  $x=0$  is mechanically oscillated without heat input from outside. This is the case in the usual acoustic experiments using a piezoelectric transducer [18]. Carlès and Zappoli found a unique response at low frequencies  $\omega t_1 \ll 1$  for isothermal boundary walls [36] [see text following Eq. (3.22)].

Let  $u_w(\propto e^{i\omega t})$  be a small applied displacement amplitude; then, to linear order in the deviations we set

$$v = i\omega u_w \quad (3.19)$$

at  $x=0$  in Eq. (2.12). Assuming Eq. (2.30) and using Eq. (3.8) we obtain

$$\begin{aligned} \beta &= - \left[ 1 + \frac{\kappa}{a_w} \sqrt{\frac{D}{i\omega}} \right] \frac{\kappa R_T}{1 - \gamma D \kappa^2 / i\omega} \rho u_w \\ &= (\gamma - 1)^{-1} \sqrt{i\omega / D X_v} R_T \rho u_w, \end{aligned} \quad (3.20)$$

where the first line is general and the second line is the approximation under the adiabatic condition, Eq. (2.34). Since the response is proportional to  $R_T$ , resonance occurs as in the previous case of temperature oscillation.

In the low-frequency case  $\omega \ll c/L$ , the interior density change is nearly homogeneous and

$$\delta \rho \cong 2\beta \cong \left[ 1 - \frac{1}{\sqrt{i\omega t_1} X_v + 1} \right] \frac{\rho u_w}{L}, \quad (3.21)$$

which is the counterpart of Eq. (3.14). As discussed below Eq. (3.16),  $\sqrt{i\omega t_1} X_v$  is large in the relatively high-frequency range  $\omega \gg 1/t_1'$  under Eq. (3.17). Thus the interior density deviation behaves as

$$\begin{aligned} \delta \rho &\cong \rho u_w / L \quad (1/t_1' \ll \omega \ll c/L) \\ &\cong \sqrt{i\omega t_1} X_v \rho u_w / L \quad (\omega \ll 1/t_1'), \end{aligned} \quad (3.22)$$

below Eq. (3.17). The volume change mostly occurs in the bulk region for  $1/t_1' \ll \omega \ll c/L$  and in the thermal diffusion layers for  $\omega t_1' \ll 1$ . The latter low-frequency regime is widened in near-critical fluids where  $t_1'$  becomes short [36].

## 3. Heat flux oscillation

In the third example, we supply a heat flux  $\dot{Q}_0 = -\lambda(dT/dx)_{x=0} \propto e^{i\omega t}$  at  $x=0$  assuming the boundary condition (2.30). It is convenient to introduce a dimensionless response function  $R_Q$  by

$$\beta = \frac{\rho}{cT} \left( \frac{\partial T}{\partial p} \right)_s R_Q \dot{Q}_0. \quad (3.23)$$

Then Eqs. (2.26) and (3.8) give

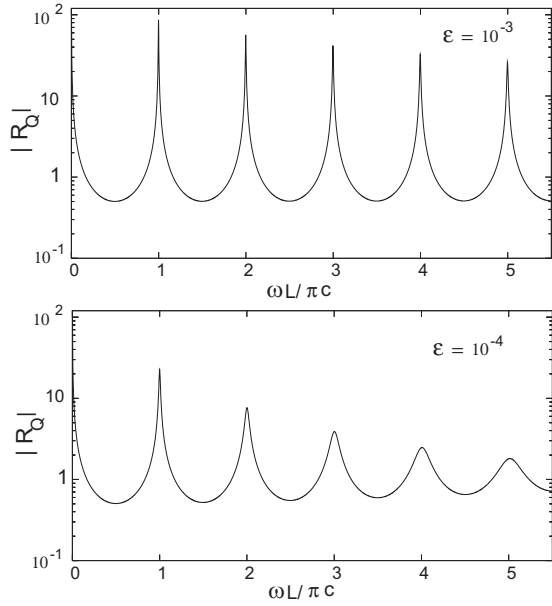


FIG. 5. Absolute value of the response function  $R_Q(\omega)$  in Eq. (3.24) vs  $\omega L/\pi c$  on a semilogarithmic scale for  $\epsilon=10^{-3}$  (upper panel) and  $10^{-4}$  (lower panel) applicable for  $\text{CO}_2$  in a Cu cell with  $L=1$  cm.

$$R_Q = \frac{ick/D}{(1 + \gamma\Delta_v)(k^2 + \kappa^2)(1 - Ze^{-2ikL})}$$

$$= \frac{1}{(1 + \Delta_v)^{3/2}(1 - Ze^{-2ikL})}, \quad (3.24)$$

where the first line is general and the second line holds under the adiabatic condition (2.34). In the complex  $\omega$  plane,  $R_Q$  has poles  $\omega'_n$ , which are equal to  $\omega_{2n}$  in Eq. (3.5) with system length changed to  $2L$ . Thus  $R_Q$  grows for  $\omega \cong n\pi c/L$  for  $\omega < (2A_B)^{-1/2}\pi c/L$ . In Fig. 5, we plot the absolute value  $|R_Q|$  as a function of  $\omega L/\pi c$  for  $\epsilon=10^{-3}$  and  $10^{-4}$ . We can see that  $|R_Q|$  is larger than  $|R_T|$  in Fig. 4 roughly by two orders of magnitude except at very low frequencies.

The behavior of  $R_Q$  in the low-frequency range  $\omega \ll c/L$  is very different from that of  $R_T$ , however. From the second line of Eq. (3.24) we have  $R_Q \cong 1/(2ikL + 2W)$  to obtain the counterpart of Eq. (3.15),

$$R_Q \cong \frac{X_v}{2\sqrt{i\omega t_2}} [1 + 2\sqrt{i\omega t_1} X_v]^{-1}. \quad (3.25)$$

Under Eq. (3.17) we find that  $R_Q \cong (1 + a_w^{-1})/2\sqrt{i\omega t_2}$  for  $\omega \ll 1/t'_1$  and  $R_Q \cong 1/4i\omega\sqrt{t_1 t_2}$  for  $1/t'_1 \ll \omega \ll c/L$ .

In this situation we may calculate the heat flux  $\dot{Q}_L$  at  $x=L$ . From Eq. (2.26) it is written as

$$\dot{Q}_L = \frac{(1-Z)e^{-ikL}}{1 - Ze^{-2ikL}} \dot{Q}_0, \quad (3.26)$$

which vanishes for  $Z=1$  (or for  $a_w=0$ ) and becomes small with increasing  $\delta_B L$ . Near the resonance frequency  $n\pi c/L$ , the ratio  $\dot{Q}_L/\dot{Q}_0$  behaves as  $(-1)^n W/[i(\omega L/c - n\pi)$

$+n\pi\zeta/2\rho c^2 + W]$ . The low-frequency behavior for  $\omega \ll c/L$  is given by

$$\dot{Q}_L = (1 + 2\sqrt{i\omega t_1} X_v)^{-1} \dot{Q}_0. \quad (3.27)$$

From the discussion below Eq. (3.16), we find  $\dot{Q}_L \cong \dot{Q}_0$  for  $\omega t'_1 \ll 1$  under Eq. (3.17). That is, an applied heat flux passes through a near-critical fluid on the time scale of  $t'_1$  under Eq. (3.17), due to the piston effect.

### C. Thermal and mechanical piston effects

#### 1. Boundary temperature change

In the original papers of the piston effect [3], the boundary temperatures at  $x=0$  and  $L$  were both raised by a common small amount  $T_1$  at  $t=0$ . Subsequently, the boundary temperatures were held fixed for  $t>0$ . In this paper, we examine the effects of finite  $a_w^{-1}$  [14,18] and large  $\zeta$  [16,17]. We suppose that the system was in equilibrium for  $t<0$  and the temperature in the wall region  $x<0$  was instantaneously raised by  $T_1$  at  $t=0$  without external heat input in the other wall region  $x>L$ . The boundary conditions are then given by  $\delta T(x,t) \rightarrow T_1$  as  $x \rightarrow -\infty$  and  $\delta T(x,t) \rightarrow 0$  as  $x-L \rightarrow \infty$  for  $t>0$ . All the deviations vanish for  $t<0$ .

The Fourier transformation of the interior temperature deviation  $\delta T(x,t)$  with respect to  $t$  is given by Eq. (3.13) with  $T_w = T_1 e^{i\omega t}/i\omega$  (since  $\int_0^\infty dt e^{-i\omega t} = 1/i\omega$ ). The inverse Fourier transformation gives

$$\frac{\delta T(x,t)}{T_1} = \int \frac{d\omega e^{i\omega t}}{2\pi i \omega} (e^{-ikx} + Ze^{ikx-2ikL}) R_T, \quad (3.28)$$

where the integration is in the range  $[-\infty, \infty]$ . Under Eq. (2.34),  $W = W(\omega)$  and  $R_T = R_T(\omega)$  are given by Eqs. (2.40) and (3.12), respectively. The integrand is analytic (without singularities) in the lower half plane  $\text{Im } \omega < 0$  and hence the integral is nonvanishing only for  $t>0$ .

In the time region  $t \gg L/c$  we may neglect the space dependence of  $\delta T(x,t)$  in the interior and use the simple expression (3.15) for  $R_T(t)$ . It then follows

$$\delta T(t) = T_1 \Psi(t)/2, \quad (3.29)$$

where we introduce the dimensionless relaxation function  $\Psi(t)$ . Its Fourier transformation reads

$$\int_0^\infty dt e^{-i\omega t} \Psi(t) = \frac{1}{i\omega(\sqrt{i\omega t_1} X_v + 1)}. \quad (3.30)$$

The inverse Fourier transformation of the right-hand side of Eq. (3.30) may be transformed into an integral along the positive imaginary axis  $\text{Im } \omega > 0$ . With  $X_v$  being defined by Eq. (2.41), we find  $\Psi(t) > 0$  for  $t > 0$ ,  $\Psi(t) \cong t/\sqrt{t_1 t_B}$  as  $t \rightarrow 0$ , and  $\Psi(t) = 1 - (t'_1/\pi t)^{1/2} + \dots$  as  $t \rightarrow \infty$ . In particular, not very close to the critical point, we may neglect the bulk viscosity and take the limit  $t_B \rightarrow 0$ ; then,  $X_v \rightarrow 1 + a_w^{-1}$  and  $\Psi(t) \rightarrow \Psi_0(s)$ , where  $\Psi_0(s)$  is a universal function of  $s = t/t'_1$  expressed as [3]

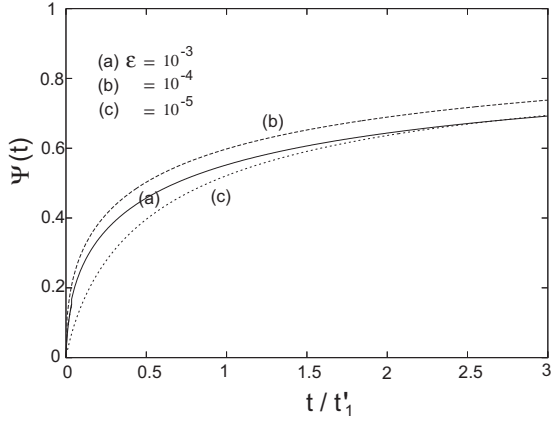


FIG. 6. Relaxation function  $\Psi(t)$  in Eq. (3.29) defined by Eq. (3.30) vs  $t/t'_1$  at  $\epsilon=10^{-3}$ ,  $10^{-4}$ , and  $10^{-5}$  for  $\text{CO}_2$  in a Cu cell with  $L=1$  cm, which is applicable for  $t \gg L/c$ . The time  $t'_1$  is defined by Eq. (3.16). The functional form of  $\Psi(t)$  as a function of  $t/t'_1$  is not sensitive to  $\epsilon$  under Eq. (3.17).

$$\Psi_0(s) = 1 - \int_0^\infty \frac{du}{\pi\sqrt{u}} \frac{e^{-us}}{1+u} = 1 - e^s \operatorname{erfc}(\sqrt{s}), \quad (3.31)$$

where  $\operatorname{erfc} = 1 - \operatorname{erf}$  is the complementary error function and  $\Psi_0 \cong 2(s/\pi)^{1/2}$  for  $s \ll 1$  and  $\Psi_0 \cong 1 - 2(\pi s)^{-1/2}$  for  $s \gg 1$ .

In Fig. 6, we display  $\Psi(t)$  as a function of  $t/t'_1$  at  $\epsilon = 10^{-3}$ ,  $10^{-4}$ , and  $10^{-5}$  for  $\text{CO}_2$  in a Cu cell with  $L=1$  cm. For  $\epsilon=10^{-3}$  we can see  $\Psi(t) \cong \Psi_0(t/t'_1)$ , where  $t_B/t'_1 \sim 0.02$  from Table I. The discussion below Eq. (3.16) indicates that  $\Psi(t)$  approaches unity on the time scale of  $t'_1$  as long as Eq. (3.17) is satisfied. This is the case even for  $\epsilon=10^{-5}$ , where  $t_B/t'_1 \cong 21$  from Table I. In fact, if  $t_B/t'_1 \gg 1$  and  $a_w \ll 1$ , we may set  $\sqrt{i\omega t_1} X_v \cong i\omega \sqrt{t_1 t_B} + a_w^{-1} \sqrt{i\omega t_1}$ , where the second term is relevant in  $\Psi(t)$  under Eq. (3.17), again leading to  $\Psi(t) \cong \Psi_0(t/t'_1)$  for  $t > a_w^2 t_B$ . However, the reverse condition of Eq. (3.17) holds extremely close to the critical point, where  $R_T \cong 1/[i\omega \sqrt{t_1 t_B} + 1]$  holds yielding [17]

$$\Psi(t) \cong 1 - \exp(-t/\sqrt{t_1 t_B}). \quad (3.32)$$

The new relaxation time  $\sqrt{t_1 t_B}$  here grows as  $\sqrt{t_1 t_B} \cong 1.0 \times 10^{-4} L \epsilon^{-0.64}$  s for near-critical  $\text{CO}_2$ .

Assuming the isothermal boundary ( $a_w = \infty$ ), Carlès and Dadzie examined the bulk viscosity effect in the thermal equilibration [17]. Their relaxation function is obtained if we set  $X_v = (1 + i\omega t_B)^{1/2}$  in Eq. (3.30). Then a new viscous regime appears for  $t_1 \gg t_B$  with  $\Psi(t)$  being given by Eq. (3.32), while the usual piston regime is encountered for  $t_1 \ll t_B$ . For  $\text{CO}_2$  we have  $t_B/t_1 \cong 2.7 \times 10^{-20} L^{-2} \epsilon^{-4.63}$ , so  $t_1 = t_B$  holds at  $\epsilon \cong 0.6 \times 10^{-4}$  with  $L=1$  cm. In our calculations based on Eq. (3.17), the different predictions have arisen from the reduced temperature dependence of  $a_w$  or the crossover of the boundary condition into the insulating one.

## 2. Volume change

We suppose a volume change by moving the boundary wall at  $x=0$  by a small length  $u_1$  instantaneously at  $t=0$  [1]. We assume the thermal boundary conditions (2.28) and

(2.30) at  $x=0$  and  $L$ . As in Eq. (3.26), the complete interior density deviation is the inverse Fourier transformation of Eq. (3.8), where  $\beta$  is given by Eq. (3.20) with  $u_w = u_1 e^{i\omega t}/i\omega$ .

Here we are interested in the late stage  $t \gg L/c$ , where the interior deviations depend only on  $t$ . The inverse Fourier transformation of Eq. (3.21) gives the interior deviations,

$$\delta\rho(t) = b_s \delta T(t) = [1 - \Psi(t)] \rho u_1 / L, \quad (3.33)$$

where  $\Psi(t)$  defined by Eq. (3.30) represents the effect of the thermal diffusion layers at  $x=0$  and  $L$ . The above form with  $\Psi = \Psi_0$  was derived in Ref. [1]. If  $u_1 > 0$ , the interior is adiabatically heated by  $b_s^{-1} \rho u_1 / L$  on the acoustic time scale  $L/c$  after the volume change, while the boundary wall temperature is almost unchanged. Subsequently, the thermal diffusion layers become effective as reverse pistons and the interior temperature deviation decays as  $(t'_1/t)^{1/2}$ .

The reverse piston effect itself generally occurs on the time scale of  $t'_1$  after a near-critical fluid was adiabatically heated or cooled. Miura *et al.* observed such a process after a pulselike heat input (see Fig. 2 in Ref. [20]).

## D. Emission of sound

We examine sound emission by mechanical and thermal pistons in the one-dimensional geometry. We neglect the incoming wave reflected at the other end  $x=L$  and consider the semi-infinite limit  $L \rightarrow \infty$ .

### 1. Boundary motion

The problem is simple in the case of boundary wall motion at  $x=0$ . If the motion is much slower than  $t_\xi$ , an emitted sound propagates with the velocity  $c$  and integration of the continuity equation  $\partial \delta\rho / \partial t = -\rho \partial v / \partial x$  simply gives the acoustic density deviation,

$$\delta\rho(x,t) = \rho v_1(t - x/c)/c, \quad (3.34)$$

where  $v_1(t) = \lim_{x \rightarrow 0} v(x,t)$  is the velocity of the boundary. The localized part of the density deviation [the term proportional to  $a$  in Eq. (2.20)] is small when differentiated with respect to time.

We may derive this relation in our theory. In fact, under the adiabatic condition (2.34), Eqs. (3.12) and (3.20) lead to

$$\beta = \frac{1 + Z}{2(1 + \Delta_v)c} i\omega \rho u_w, \quad (3.35)$$

for  $e^{-2ikL} \rightarrow 0$ . If we set  $1 + \Delta_v \cong 1$  and  $Z \cong 1$ , the above relation becomes  $\beta \cong i\omega \rho u_w / c$ , leading to Eq. (3.34). Here  $i\omega u_w$  is the Fourier transformation of  $v_1(t)$  multiplied by  $e^{i\omega t}$ . Thus Eq. (3.34) holds on time scales longer than  $t_\xi$  [even when the time scale of  $v_1(t)$  is shorter than  $t_B$ ].

### 2. Heat input

A sound is also emitted when a time-dependent heat flux  $\dot{Q}_0(t)$  is supplied at the boundary at  $x=0$ . We assume  $\dot{Q}_0(t) = 0$  for  $t < 0$ . From Eq. (3.8) the Fourier transformation of the interior density deviation  $\delta\rho(x,t)$  is of the form  $\beta e^{ikx}$  with  $\beta$  being given by Eq. (3.23). Under the adiabatic condition

(2.34) we may use the second line of Eq. (3.24). The inverse Fourier transformation gives the convolution relation,

$$\delta\rho(x,t) = \frac{\rho}{cT} \left( \frac{\partial T}{\partial p} \right)_s \int_0^t d\tau \Phi(x,t-\tau) \dot{Q}_0(\tau). \quad (3.36)$$

The memory function  $\Phi(x,t)$  is defined for  $t > 0$  as

$$\Phi(x,t) = \int \frac{d\omega}{2\pi} \frac{c^3}{c^*(\omega)^3} e^{i\omega t - ikx}, \quad (3.37)$$

where  $c^*(\omega) = c(1 + \Delta_v)^{1/2}$  from Eq. (2.39) and  $k = \omega/c^*(\omega)$ . The time integration of this function is normalized as  $\int_0^\infty dt \Phi(x,t) = 1$ .

From the integration in the region  $\omega < t_\xi^{-1}$  we obtain the long-time behavior  $\Phi(0,t) \equiv (4t/\pi t_\xi^3)^{1/2} e^{-t/t_\xi}$  with  $t_\xi \equiv R_B t_\xi$  at  $x=0$ . Since this relaxation is exponential, we may set  $\Phi(0,t) \equiv \delta(t)$  ( $\delta$  function) at  $x=0$  on time scales longer than  $t_\xi$  or when  $\dot{Q}_0(t)$  varies slower than  $t_\xi$ . Furthermore, if the distance  $x$  is not large such that the bulk damping is negligible at the position  $x$ , we may set  $\Phi(x,t) \equiv \delta(t-x/c)$  to find the simple formula for the emitted sound,

$$\delta\rho(x,t) = \frac{\rho}{cT} \left( \frac{\partial T}{\partial p} \right)_s \dot{Q}_0(t-x/c), \quad (3.38)$$

as the counterpart of Eq. (3.34). On the other hand, use of Eq. (A6) gives the short-time behavior [1],

$$\Phi(0,t) = (\hat{\alpha}/2\hat{v})(t/t_\xi)^{\hat{\alpha}/2\hat{v}}/t, \quad (3.39)$$

valid in the time region  $t \lesssim t_\xi$  with  $\hat{\alpha}/2\hat{v} \equiv 0.088$  (see the Appendix). This behavior could be detectable only for rapid variations of  $\dot{Q}_0$  within a time shorter than  $t_\xi$ .

Miura *et al.* applied a stepwise heat flux with  $\dot{Q} = 0.183 \times 10^7$  from a film heater slightly separated from the upper boundary to find a stepwise outgoing sound with  $\delta\rho/\rho \equiv 2.2 \times 10^{-7}$ , where  $\dot{Q}$  is in cgs units (erg/cm<sup>2</sup>s) [20]. Our theoretical expression (3.38) becomes  $\delta\rho/\rho = 1.38 \times 10^{-13} \dot{Q}$  with the aid of  $(\partial T/\partial p)_s \equiv T_c/6.98\rho_c$  for CO<sub>2</sub> [37]. For their experimental  $\dot{Q}$  our theory gives  $\delta\rho/\rho = 2.55 \times 10^{-7}$  in fair agreement with the observed density change. Furthermore, they could generate sound pulses with duration of order 10  $\mu$ s by applying short-time heat input. They were interested in the adiabatically increased energy  $E_{\text{ad}} \equiv p \int dx \delta\rho(x,t)/\rho$  in the pulse region per unit area. Here Eq. (3.38) yields [3]

$$E_{\text{ad}} = \frac{p}{T} \left( \frac{\partial T}{\partial p} \right)_s Q, \quad (3.40)$$

where  $Q = \int dt \dot{Q}(t)$  is the total heat supplied (per unit area). The ratio  $E_{\text{ad}}/Q$  represents the efficiency of transforming applied heat to mechanical work. Theoretically, it is given by  $(\partial T/\partial p)_s p/T \equiv (\partial T/\partial p)_{\text{cs}} p_c/T_c$  as in Eq. (3.40) and is equal to  $1/6.98 = 0.14$  for near-critical CO<sub>2</sub> [37]. The measured values of the ratio  $E_{\text{ad}}/Q$  at the first pulse arrival to the detector were in the range 0.11–0.12 again in fair agreement with our theory.

We may calculate the excess mass density  $\Delta M_a \equiv \int_0^\infty dx \delta\rho(x,t)$  (per unit area) in the outgoing wave emitted from the boundary at  $x=0$ . From Eq. (3.38) we obtain  $\delta M_a = \rho(\partial T/\partial p)_s Q_0(t)/T$  for heating slower than  $t_\xi$  in terms of the heat supply  $Q_0(t) = \int_0^t dt' \dot{Q}_0(t')$ . If this expression is divided by the system length  $L$ , it becomes of the same form as that for the interior density change in Eq. (1.2). Note that Eq. (1.2) holds on time scales much longer than the acoustic time  $t_a = L/c$ . Here we argue how Eq. (1.2) can be obtained starting with the emission law (3.38) [20]. That is, we supply a heat  $\dot{Q}(t)$  per unit time to the fluid. If it changes slowly compared to  $t_a$ , we may suppose a time interval with width  $\delta t \gg t_a$  in which  $\dot{Q}(t)$  is almost unchanged. Since  $\delta t/t_a$  is the traversal number much larger than unity, the adiabatic pressure and density increases in the interior region are the superposition of many steps given by

$$\delta\rho = \frac{\delta p}{c^2} = \frac{\delta t}{t_a} \frac{\rho}{cT} \left( \frac{\partial T}{\partial p} \right)_s \dot{Q}. \quad (3.41)$$

This relation is equivalent to Eq. (1.2) in terms of the incremental heat supply  $\delta Q = \dot{Q} \delta t$ .

### E. Reflection of sound

Reflection of plane wave sounds is discussed for an isothermal rigid boundary in the textbook of Landau-Lifshitz [30]. Miura *et al.* [20] generated pulses with duration shorter than  $L/c$ , which were reflected at the walls and their shapes gradually flattened. However, the damping of such short pulses upon reflection was very large even not very close to the critical point, which cannot be explained by our one-dimensional theory in the following (see the last paragraph in this section). They also generated stepwise pulses with duration longer than  $L/c$ . Carlès [21] excellently reproduced time evolution of such long pulses at  $T - T_c = 150$  mK ( $\epsilon = 0.5 \times 10^{-3}$ ), assuming the isothermal boundaries and neglecting the bulk viscosity.

We consider a pulse approaching to the boundary at  $x=0$  in the semi-infinite limit  $L \rightarrow \infty$ . Reflection takes place upon its encounter with the wall. The density deviations of the incoming and outgoing pulses are obtained as the inverse Fourier transformation of Eq. (2.20). Neglecting the bulk damping in the neighborhood of the boundary, we may express them as  $\rho_i(t+x/c)$  and  $\rho_o(t-x/c)$ , respectively. Using  $\alpha(\omega) = e^{i\omega t} \int d\tau e^{-i\omega\tau} \rho_i(\tau)$  and  $\beta = Z\alpha$ , we obtain

$$\rho_o(t) = \int \frac{d\omega}{2\pi} \int dt' Z(\omega) e^{i\omega(t-t')} \rho_i(t'). \quad (3.42)$$

The interior density deviation is the sum  $\delta\rho(x,t) = \rho_i(t+x/c) + \rho_o(t-x/c)$ . Since  $Z(0) = 1$ , the excess mass  $\Delta M$  per unit area is invariant upon reflection as

$$\Delta M = c \int dt \rho_i(t) = c \int dt \rho_o(t). \quad (3.43)$$

This relation holds if we integrate a long tail of the reflected pulse  $\rho_o(t)$  at large  $t$  [see Eq. (3.48)].

If  $\rho_i(t)$  changes much slower than  $t_\xi$ , we may set  $Z \cong 1 - 2W$  with  $W = (\gamma - 1)\sqrt{i\Delta_T}/X_v$  from Eq. (2.40). In this approximation we may rewrite Eq. (3.42) in the following convolution form:

$$\begin{aligned}\rho_o(t) &= \rho_i(t) - \int_0^\infty d\tau \dot{\chi}(\tau) [\rho_i(t - \tau) - \rho_i(t)] \\ &= \rho_i(t) - \int_0^\infty d\tau \chi(\tau) \dot{\rho}_i(t - \tau),\end{aligned}\quad (3.44)$$

where  $\dot{\chi}(t) = \partial\chi(t)/\partial t$  and  $\dot{\rho}_i(t) = \partial\rho_i(t)/\partial t$ . From Eq. (3.42) the function  $\chi(t)$  is the inverse Fourier transformation of  $(1 - Z)/i\omega \cong 2W/i\omega$ . Some calculations (in the complex  $\omega$  plane) give  $\chi(t)$  in the integral form,

$$\chi(t) = \varepsilon_r \int_0^\infty \frac{d\Omega}{\pi\sqrt{\Omega}} \operatorname{Re} \left[ \frac{e^{-\Omega s}}{a_w^{-1} + \sqrt{1 - \Omega}} \right], \quad (3.45)$$

where  $s = t/t_B$  is the scaled time,  $\operatorname{Re}[\cdot]$  denotes taking the real part, and  $\sqrt{1 - \Omega} = i\sqrt{\Omega - 1}$  for  $\Omega > 1$ . The dimensionless parameter  $\varepsilon_r$  is defined by

$$\varepsilon_r = 2(\gamma - 1)\sqrt{D/c^2 t_B}, \quad (3.46)$$

which decreases near the critical point as  $\varepsilon_r \cong 4.3\epsilon^{0.75}$  for  $\text{CO}_2$ . The function  $\chi(t)$  depends only on  $s$  and  $a_w$ . For  $a_w \gg 1$  we have  $\chi(t)/\varepsilon_r \cong e^{-s/2} I_0(s/2)$  with  $I_0$  being the modified Bessel function, while for  $a_w \ll 1$  we have  $\chi(t)/\varepsilon_r \cong 1 - \Phi_0(s/a_w^2)$  with  $\Phi_0$  being defined by Eq. (3.31). Thus  $\chi(t)$  changes on the scale of  $t'_B$  in Eq. (2.42) and its limiting behaviors are as follows:

$$\begin{aligned}\frac{\chi(t)}{\varepsilon_r} &= (1 + a_w^{-1})^{-1} (\pi s)^{-1/2} + \dots \quad (s \rightarrow \infty) \\ &= 1 - 2a_w^{-1} (s/\pi)^{1/2} + \dots \quad (s \rightarrow 0).\end{aligned}\quad (3.47)$$

In addition, the second term of Eq. (3.43) representing the distortion is negative (positive) when  $\rho_i(t)$  is increasing (decreasing). This initial drop is because of heating and expansion of the pulse at the boundary.

From the first line of Eq. (3.47) we obtain  $\dot{\chi}(t) \cong -(t_2/\pi)^{1/2} t^{-3/2}$  for  $t \gg t'_B$ . (i) Let  $\rho_i(t)$  be peaked in the region  $|t| < t_w$  with  $t_w$  being the pulse duration time; then, for  $t \gg t'_B$  and  $t_w$ , the first line of Eq. (3.44) gives a long-time tail of the reflected wave,

$$[\rho(t)]_{\text{tail}} = \frac{\Delta M}{c} (t_2/\pi)^{1/2} t^{-3/2}, \quad (3.48)$$

where  $\Delta M$  is the total excess mass defined by Eq. (3.43). If  $t > t_w > t'_B$ , the excess mass behind the peak in the form of sound is given by the time integral of the tail (3.47) in the region  $[t_w, t]$  multiplied by  $c$ . Dividing it by  $\Delta M$  we obtain the fraction of the excess mass behind the peak at time  $t(>t_w)$  [38],

$$[\Delta M(t)]_{\text{tail}}/\Delta M = (4t_2/\pi t_w)^{1/2} - (4t_2/\pi t)^{1/2}, \quad (3.49)$$

which is equal to  $10^{-7} \epsilon^{-0.75} (t_w^{-1/2} - t^{-1/2})$  (with  $t_w$  and  $t$  in seconds) for  $a_w \gg 1$  in  $\text{CO}_2$ . (ii) As another example, we con-

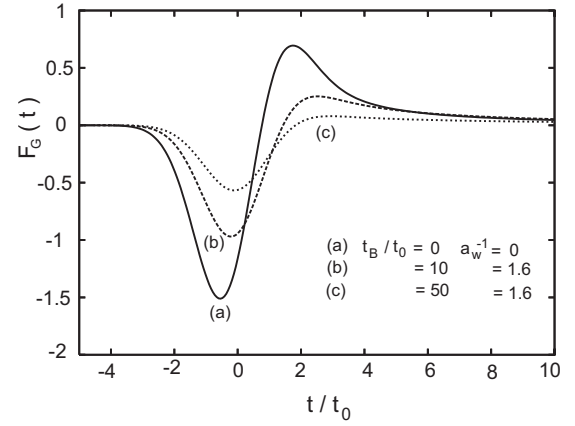


FIG. 7. Scaled pulse deformation  $F_G(t) \propto \rho_o(t) - \rho_i(t)$  defined by Eq. (3.51) vs scaled time  $t/t_w$  for a Gaussian incoming pulse with width  $t_w$ . Here  $t_B/t_w \rightarrow 0$  and  $a_w = \infty$  (a),  $t_B/t_w = 10$  and  $a_w = 0.63$  (b), and  $t_B/t_w = 50$  and  $a_w = 0.63$  (c).

sider a stepwise change, where  $\rho_i(t)$  is equal to 0 for  $t < 0$  and to a constant  $\rho_1$  for  $t > t_w$  with  $t_w$  being the transient time here. Then, for  $t \gg t'_B$  and  $t_w$ , the second line of Eq. (3.44) gives a longer tail,

$$[\rho(t)]_{\text{tail}} = \rho_1 (4t_2/\pi)^{1/2} t^{-1/2}. \quad (3.50)$$

The bulk viscosity does not appear in these tails.

When  $\rho_i(t)$  changes much slower than  $t'_B$ , only the long-time behavior of  $\chi(t)$  is relevant in  $\rho_o(t)$ . From Eq. (3.44) we find the following convolution relations:

$$\begin{aligned}\rho_o(t) &= \rho_i(t) + \sqrt{\frac{t_2}{\pi}} \int_0^\infty \frac{d\tau}{\tau^{3/2}} [\rho_i(t - \tau) - \rho_i(t)] \\ &= \rho_i(t) - \sqrt{\frac{4t_2}{\pi}} \int_0^\infty \frac{d\tau}{\sqrt{\tau}} \dot{\rho}_i(t - \tau),\end{aligned}\quad (3.51)$$

from which the long-time tails (3.48) and (3.50) readily follow. The above expressions contain only  $t_2$  in Eq. (2.44) and not  $t_B$ . They are applicable far from the critical point (where  $t_B$  becomes short). With decreasing  $\epsilon$  for the isothermal boundary ( $a_w > 1$ ),  $t_2$  grows and the distortion of the reflected pulse increases as long as the pulse width is longer than  $t_B$ . However, if the pulse width is shorter than  $t'_B$ , the distortion decreases on approaching the critical point since  $\varepsilon_r$  in Eq. (3.46) decreases.

As a simple illustration, let us consider a Gaussian pulse  $\rho_i(t) = \rho_1 \exp(-t^2/2t_w^2)$ , where  $\rho_1$  is the pulse height and  $t_w$  is the pulse width. Since its Fourier transformation is  $(2\pi)^{1/2} \rho_1 t_w e^{-\omega^2 t_w^2/2}$ , we may readily calculate  $\rho_o(t)$ . In Fig. 7, we plot the normalized pulse deformation defined by

$$F_G(t) = [\rho_o(t) - \rho_i(t)] / (\rho_1 \sqrt{t_2/t_w}). \quad (3.52)$$

The curve (a) is for the limiting case  $t_B/t_w \rightarrow 0$  and  $a_w = \infty$ , while  $t_B/t_w = 10$  and  $a_w = 0.63$  in (b), and  $t_B/t_w = 50$  and  $a_w = 0.63$  in (c). In Table I we have  $a_w = 0.63$  and  $t_B = 1.9$  msec at  $\epsilon = 10^{-4}$  for  $\text{CO}_2$  in a Cu cell, where pulses with  $t_w \ll t_B$  are well possible [20]. We recognize that the distortion is nega-

tive for  $t \lesssim t_w$  and is positive for  $t \gtrsim t_w$  [in accord with the comment below Eq. (3.47)] and that the distortion is decreased as  $t_B/t_w$  is increased or for shorter pulses due to the bulk viscosity growth.

In the short-pulse experiment at  $T - T_c = 500$  mK ( $\epsilon = 1.6 \times 10^{-3}$ ) [20], the boundaries should be isothermal and the bulk viscosity should be negligible in the thermal diffusion layers. There, the pulse duration time  $t_w$  was about  $5 \mu\text{K}$ ; then, the factor  $(t_w/t_2)^{1/2}$  in the denominator of Eq. (3.52) is of order 0.01. However, even at this relatively large reduced temperature, the observed pulse deformation was of order 10%, which is much larger than predicted by our one-dimensional theory neglecting side wall effects.

#### IV. SUMMARY AND REMARKS

In summary, we have examined various thermoacoustic effects in one-component supercritical fluids in a one-dimensional geometry. We summarize our main results.

(i) In the linear hydrodynamics, sound modes and thermal diffusion modes are both present as in Eq. (2.20), depending on given boundary conditions. The latter modes can be absent only for the insulating boundary condition  $a_w = 0$ . The calculations are straightforward and the final expressions are much simplified under the adiabatic condition (2.34) or for low frequencies  $\omega \ll c^2/\gamma D$ . It is remarkable that the bulk viscosity  $\zeta$  appears in the combination  $\omega\gamma\zeta/\rho c^2 = \omega t_B$  in  $\kappa$  in Eq. (2.36), as first pointed out by Carlès [16,17]. The resultant characteristic time  $t_B$  grows as  $\epsilon^{-3.0}$ , while the lifetime of the critical fluctuations  $t_\xi$  grows as  $\epsilon^{-1.9}$ .

(ii) We have introduced the reflection factor  $Z(\omega)$  as the ratio between outgoing and incoming sounds. Using  $Z$  or  $W = (1 - Z)/(1 + Z)$  we have examined the acoustic eigenmodes, the response of the fluid to applied oscillation of the boundary temperature, the boundary heat flux, and the boundary position. To these thermal and mechanical perturbations, resonance is induced when the frequency of the perturbation is close to one of the eigenfrequencies, while nearly uniform adiabatic changes are caused in the interior at much lower frequencies owing to the piston effect.

(iii) We have also examined the response to a stepwise change of the boundary temperature and the boundary position. The relaxation time is given by the modified piston time  $t'_1$  in Eq. (3.16) first introduced by Ferrell and Hao [14]. It is equal to the original piston time  $t_1$  in Eq. (1.1) for the isothermal boundary  $a_w \gg 1$  and to  $a_w^{-2}t_1$  for the insulating boundary  $a_w \ll 1$ .

(iv) As the critical point is approached, the role of the thermal diffusion layers is eventually diminished both by decreasing of the effusivity ratio  $a_w$  and by growing of the bulk viscosity  $\zeta$ , while the bulk sound attenuation becomes increasingly stronger. The bulk viscosity effect in the thermal diffusion layer is thus masked by its enhanced effect in the bulk. This aspect can be seen in the damping of the eigenmodes, as studied by Gillis *et al.* [18] and as in Fig. 3 in our work. It is more apparent in the behavior of  $\delta T$  and  $\delta p$  in the thermal diffusion layer in Eqs. (2.51) and (2.52).

(v) For  $\text{CO}_2$  in a Cu cell, the boundary becomes thermally insulating for  $\epsilon \ll 10^{-4}$ . Then, as long as Eq. (3.17) holds, the

bulk viscosity does not play a significant role in the thermal diffusion layers. The viscous regime predicted by Carlès and Dadzie emerges in the reverse condition or for  $\epsilon < 2 \times 10^{-6}$  with  $L = 1$  cm [16,17]. To increase this crossover reduced temperature, the cell length  $L$  needs to be shorter.

(vi) We have also examined sound emission and reflection at the boundary, which are elementary hydrodynamic processes but seem to have not been well examined even far from the critical point [30]. For emission, the formulas (3.34) and (3.38) are valid for a mechanical piston and a thermal heat input on time scales longer than  $t_\xi$ . We have given another derivation of the fundamental relation (1.2) of the piston effect from the emission rule around Eq. (3.41). For reflection, Eq. (3.44) with Eq. (3.45) holds on time scales longer than  $t_\xi$ . The formula (3.51) is the classical one valid on time scales much longer than  $t_B$ , where the distortion of the outgoing pulse increases on approaching the critical point. For pulses shorter than  $t_B$ , the distortion of the outgoing pulse is decreased as can be seen in Fig. 7.

We make some critical remarks and mention future problems below.

(i) We have neglected gravity. In experiments on earth, gravity effects become increasingly important as the critical point is approached. It is noteworthy that stirring has been used to remove gravity-induced density stratification [18,39]. See Refs. [1,40] for theories of such stirring effects.

(ii) We have used linearized hydrodynamic equations. However, as the critical point is approached, nonlinear theory is needed except for extremely small perturbations. This aspect has not yet been well understood except for some special cases [3].

(iii) In this paper, we have treated near-critical fluids in one-phase states. The present work should be extended to the case of two-phase coexistence. On long time scales conversion between gas and liquid at an interface gives rise to slow thermal relaxation [3,41], while on acoustic time scales sound reflection and transmission at an interface are still not understood [42]. Also challenging is two-phase hydrodynamics, where latent heat transport and wetting dynamics come into play in addition to the piston effect [42–44].

#### ACKNOWLEDGMENTS

I would like to thank the members of the experimental group of the piston effect in Japan [20], Takeo Satoh, and P. Carlès for valuable discussions. Thanks are also due to Horst Meyer, K. A. Gillis, and M. R. Moldover for informative correspondence. This work was supported by grants from the Japan Space Forum and from the 21st Century COE project (Center for Diversity and Universality in Physics) from the Ministry of Education, Culture, Sports, Science and Technology of Japan.

#### APPENDIX: SUMMARY OF CRITICAL BEHAVIOR

Let a one-component fluid be on the critical isochore ( $\rho = \rho_c$ ) with small positive  $\epsilon = T/T_c - 1$  near the gas-liquid critical point. The physical parameters used in Table I and the figures are given below. Hereafter  $\hat{\nu} (\cong 0.63)$ ,  $\hat{\gamma} (\cong 1.24)$ , and

$\hat{\alpha}(\cong 0.10)$  are the usual critical exponents. Data of near-critical CO<sub>2</sub> can be found in Refs. [31,37], where  $T_c = 304.12$  K. Theories of the dynamic critical behavior are summarized in Ref. [1].

Our hydrodynamic description is valid when the spatial scale under investigation is longer than the correlation length  $\xi = \xi_0 \epsilon^{-\hat{\nu}}$ , where  $\xi_0 = 1.5$  Å for CO<sub>2</sub>. The constant-volume specific heat  $C_V = \rho T (\partial s / \partial T)_\rho$  and the isobaric specific heat  $C_p = \rho T (\partial s / \partial T)_p$  are expressed as

$$C_V = A_V [\epsilon^{-\hat{\alpha}} + B], \quad C_p = A_p \epsilon^{-\hat{\gamma}}. \quad (\text{A1})$$

The background part of  $C_p$  is neglected. For CO<sub>2</sub> on the critical isochore, the coefficients are given by  $A_V = 26.3 k_B n^*$ ,  $B = -0.9$ , and  $A_p = 2.58 k_B n^*$ , where  $n^* = \rho_c / k_B T_c \cong 1.76 \times 10^{21}$  cm<sup>-3</sup>. The specific-heat ratio  $\gamma$  grows strongly as  $\gamma_0 \epsilon^{-\hat{\gamma} + \hat{\alpha}}$  if the background ( $\propto B$ ) of  $C_V$  is neglected, where  $\gamma_0 = 0.1$  for CO<sub>2</sub>. As discussed below Eq. (2.9), the sound velocity  $c$  (at zero frequency) may be approximated as

$$c^2 = T (\partial p / \partial T)_{c_x}^2 / \rho C_V, \quad (\text{A2})$$

so  $c^2 = c_0^2 \epsilon^{\hat{\alpha}} / (1 + B \epsilon^{\hat{\alpha}})$  with  $c_0^2 = T (\partial p / \partial T)_{c_x}^2 / \rho A_V$ . In writing the figures in this paper, we have set  $c = 2.3 \times 10^4 \epsilon^{0.06}$  cm s<sup>-1</sup> for CO<sub>2</sub> neglecting the background of  $C_V$  [20].

The thermal conductivity  $\lambda$  grows such that the thermal diffusion constant  $D$  behaves as

$$D = \lambda / C_p = k_B T / 6 \pi \eta \xi = D_0 \epsilon^{\hat{\nu}}, \quad (\text{A3})$$

where  $D_0 = 4.0 \times 10^{-4}$  cm<sup>2</sup> s<sup>-1</sup> for CO<sub>2</sub>. The background part of  $\lambda$  is neglected, so  $\lambda \propto \epsilon^{\hat{\nu} - \hat{\gamma}}$ . The mean relaxation time of the critical fluctuations with size  $\xi$  increases as

$$t_\xi = \xi^2 / D = t_0 \epsilon^{-3\hat{\nu}}, \quad (\text{A4})$$

where  $t_0 = 0.56 \times 10^{-12}$  s for CO<sub>2</sub>. The shear viscosity  $\eta$  is only weakly singular and may be treated as a constant independent of  $\epsilon$  and  $\omega$  to make rough estimates.

On the other hand, the zero-frequency bulk viscosity  $\zeta$  grows very strongly as

$$\zeta = \rho c^2 R_B t_\xi, \quad (\text{A5})$$

where  $R_B$  is a universal number estimated to be about 0.03 [1,33]. For CO<sub>2</sub>,  $\zeta / \rho \cong 0.9 \times 10^{-5} \epsilon^{-2+2\hat{\alpha}}$  cm<sup>2</sup> s<sup>-1</sup>, so  $\zeta / \rho D = \Delta_v / \Delta_T \cong 0.02 \epsilon^{-2-\hat{\nu}+2\hat{\alpha}}$  [see Eqs. (2.13) and (2.14)]. In the high-frequency regime  $\omega t_\xi \gg 1$ ,  $\zeta$  becomes complex such that the complex sound velocity  $c^*(\omega)$  in Eq. (2.39) becomes asymptotically independent of  $\epsilon$  [32–34]. It is hence convenient to examine the high-frequency behavior of  $c^*(\omega)$ . Including the background of  $C_V$  in Eq. (A1), we may derive an approximate expression valid for  $\omega t_\xi \gg 1$  [1],

$$c^*(\omega)^2 = c_0^2 / [(i \omega t_0 / 2)^{-\hat{\alpha}/3\hat{\nu}} + B], \quad (\text{A6})$$

where  $c_0^2$  is introduced below Eq. (A2) and  $t_0$  is defined by Eq. (A4). Since  $i^{-\hat{\alpha}/3\hat{\nu}} = 1 - i\pi\hat{\alpha}/6\hat{\nu} + \dots$  from  $\hat{\alpha}/3\hat{\nu} = 0.053 \ll 1$ , we find  $0 < \text{Im } c^* \ll \text{Re } c^*$  and  $\text{Im } \Delta_v = \omega \text{Re } \zeta / \rho c^2 \ll 1$ , so that

$$\frac{\text{Im } c^*}{\text{Re } c^*} = \frac{\text{Im } \Delta_v}{2(1 + \text{Re } \Delta_v)} = \frac{\pi \hat{\alpha} / 6 \hat{\nu}}{2(1 + X)}, \quad (\text{A7})$$

where  $X \equiv B(\omega t_0 / 2)^{\hat{\alpha}/3\hat{\nu}}$ . This relation leads to Eq. (3.10) if  $X$  is neglected. The real part  $\text{Re } c^*$  represents the  $\omega$ -dependent sound velocity behaving as

$$\text{Re } c^* = c_0 (\omega t_0 / 2)^{\hat{\alpha}/6\hat{\nu}} / \sqrt{1 + X}, \quad (\text{A8})$$

which very slowly increases with increasing  $\omega$  in the region  $\omega t_\xi > 1$  (see Fig. 6.8 in Ref. [1]). The high-frequency bulk viscosity defined by  $\zeta = \rho [c^*(\omega)^2 - c^2] / i\omega$  behaves roughly as  $\omega^{-1}$ . It has a small imaginary part given by  $\text{Im } \zeta \cong -\rho [\text{Re } c^*(\omega)^2 - c^2] / \omega$ .

Furthermore, in our thermoacoustic problems, we have introduced the time  $t_B$  in Eq. (2.37), which behaves as

$$t_B = t_B^0 \epsilon^{-3\hat{\nu} - \hat{\gamma} + \hat{\alpha}}, \quad (\text{A9})$$

where  $t_B^0 = 1.7 \times 10^{-15}$  s for CO<sub>2</sub>. The effusivity ratio  $a_w$  in Eq. (2.29) decreases as

$$a_w = a_w^0 \epsilon^{\hat{\gamma} - \hat{\nu}/2}. \quad (\text{A10})$$

For  $a_w^0 \gg 1$  the boundary wall crosses over from an isothermal one to a thermally insulating one on approaching the critical point. For example, between Cu and CO<sub>2</sub>, we have  $a_w^0 = 3 \times 10^3$  [20], where  $a_w < 1$  is reached for  $\epsilon < 1.6 \times 10^{-4}$ . The  $a_w^0$  was smaller for the walls used in Refs. [15,18].

- 
- [1] A. Onuki, *Phase Transition Dynamics* (Cambridge University Press, Cambridge, 2002). In Section 6 of this book, the acoustic resonance of near-critical fluids is examined without the bulk viscosity and in the isothermal boundary condition.
- [2] K. Nitsche and J. Straub, *Proceedings of the 6th European Symposium on Material Science under Microgravity Conditions* (Bordeaux, France, 1986); J. Straub and L. Eicher, *Phys. Rev. Lett.* **75**, 1554 (1995).
- [3] A. Onuki, H. Hao, and R. A. Ferrell, *Phys. Rev. A* **41**, 2256 (1990); A. Onuki and R. A. Ferrell, *Physica A* **164**, 245 (1990).
- [4] H. Boukari, J. N. Shaumeyer, M. E. Briggs, and R. W. Gam-

mon, *Phys. Rev. A* **41**, 2260 (1990); H. Boukari, M. E. Briggs, J. N. Shaumeyer, and R. W. Gammon, *Phys. Rev. Lett.* **65**, 2654 (1990).

- [5] R. A. Wilkinson, G. A. Zimmerli, H. Hao, M. R. Moldover, R. F. Berg, W. L. Johnson, R. A. Ferrell, and R. W. Gammon, *Phys. Rev. E* **57**, 436 (1998).
- [6] B. Zappoli, D. Bailly, Y. Garrabos, B. Le Neindre, P. Guenoun, and D. Beysens, *Phys. Rev. A* **41**, 2264 (1990); P. Guenoun, B. Khalil, D. Beysens, Y. Garrabos, F. Kammoun, B. Le Neindre, and B. Zappoli, *Phys. Rev. E* **47**, 1531 (1993); Y. Garrabos, M. Bonetti, D. Beysens, F. Perrot, T. Fröhlich, P. Carlès, and B. Zappoli, *ibid.* **57**, 5665 (1998).

- [7] R. P. Behringer, A. Onuki, and H. Meyer, *J. Low Temp. Phys.* **81**, 71 (1990).
- [8] H. Klein, G. Schmitz, and D. Woermann, *Phys. Rev. A* **43**, 4562 (1991).
- [9] J. Straub, L. Eicher, and A. Haupt, *Phys. Rev. E* **51**, 5556 (1995); J. Straub and L. Eicher, *Phys. Rev. Lett.* **75**, 1554 (1995).
- [10] F. Zhong and H. Meyer, *Phys. Rev. E* **51**, 3223 (1995); A. Kogan and H. Meyer, *J. Low Temp. Phys.* **112**, 419 (1998).
- [11] F. Zhong, A. Kogan, and H. Meyer, *J. Low Temp. Phys.* **108**, 161 (1997).
- [12] B. Zappoli and A. D. Daubin, *Phys. Fluids* **6**, 1929 (1995); D. Bailly and B. Zappoli, *Phys. Rev. E* **62**, 2353 (2000).
- [13] T. Maekawa, K. Ishii, M. Ohnishi, and S. Yoshihara, *Adv. Space Res.* **29**, 589 (2002); *J. Phys. A* **37**, 7955 (2004).
- [14] R. A. Ferrell and H. Hao, *Physica A* **197**, 23 (1993).
- [15] The effusivity is defined by  $\epsilon_f \equiv (C\lambda)^{1/2} = CD^{1/2}$  for each material, where  $C$  is the isobaric specific heat per unit volume,  $\lambda$  is the thermal conductivity, and  $D = \lambda/C$  is the thermal diffusivity. For Cu used in Ref. [20],  $\epsilon_f/k_B = 2.6 \times 10^{23} \text{ cm}^{-2} \text{ s}^{-1/2}$ . In Ref. [18],  $\epsilon_f/k_B = 4.6 \times 10^{22}$  for a stainless steel resonator and  $\epsilon_f/k_B = 2.7 \times 10^{21}$  for a polymer-coated resonator in the same units. The diffusivity ratio is defined as in Eq. (2.29) in this paper.
- [16] P. Carlès, *Phys. Fluids* **10**, 2164 (1998).
- [17] P. Carlès and K. Dadzie, *Phys. Rev. E* **71**, 066310 (2005).
- [18] K. A. Gillis, I. I. Shinder, and M. R. Moldover, *Phys. Rev. E* **70**, 021201 (2004); **72**, 051201 (2005); K. A. Gillis, I. I. Shinder, and M. R. Moldover, *Phys. Rev. Lett.* **97**, 104502 (2006). In these papers they defined  $\Delta_v = \omega \nu_\ell / c^2$  and  $\Delta_T = \omega D / c^2$  without  $i$ .
- [19] M. Ohnishi, S. Yoshihara, M. Sakurai, Y. Miura, M. Ishikawa, H. Kobayashi, T. Takenouchi, J. Kawai, K. Honda, and M. Matsumoto, *Microgravity Sci. Technol.* **XVI-1**, 306 (2005).
- [20] Y. Miura, S. Yoshihara, M. Ohnishi, K. Honda, M. Matsumoto, J. Kawai, M. Ishikawa, H. Kobayashi, and A. Onuki, *Phys. Rev. E* **74**, 010101(R) (2006).
- [21] P. Carlès, *Phys. Fluids* **18**, 126102 (2006).
- [22] A. B. Kogan, D. Murphy, and H. Meyer, *Phys. Rev. Lett.* **82**, 4635 (1999); A. B. Kogan and H. Meyer, *Phys. Rev. E* **63**, 056310 (2001).
- [23] H. Azuma, S. Yoshihara, M. Onishi, K. Ishii, S. Masuda, and T. Maekawa, *Int. J. Heat Mass Transfer* **42**, 771 (1999).
- [24] T. Fröhlich, D. Beysens, and Y. Garrabos, *Phys. Rev. E* **74**, 046307 (2006).
- [25] S. Amiroudine, P. Bontoux, P. Larroud, B. Gilly, and B. Zappoli, *J. Fluid Mech.* **442**, 119 (2001).
- [26] Y. Chiwata and A. Onuki, *Phys. Rev. Lett.* **87**, 144301 (2001); A. Furukawa and A. Onuki, *Phys. Rev. E* **66**, 016302 (2002).
- [27] S. Amiroudine and B. Zappoli, *Phys. Rev. Lett.* **90**, 105303 (2003); G. Accary, I. Raspo, P. Bontoux, and B. Zappoli, *Phys. Rev. E* **72**, 035301(R) (2005).
- [28] E. B. Soboleva, *Phys. Rev. E* **68**, 042201 (2003).
- [29] G. Accary, I. Raspo, P. Bontoux, and B. Zappoli, *C. R. Mec.* **332**, 209 (2004).
- [30] L. D. Landau and E. M. Lifshitz, *Fluid Mechanics* (Pergamon, New York, 1959).
- [31] H. L. Swinney and D. L. Henry, *Phys. Rev. A* **8**, 2586 (1973).
- [32] R. A. Ferrell and J. K. Bhattacharjee, *Phys. Lett.* **86**, 109 (1981); J. K. Bhattacharjee and R. A. Ferrell, *Phys. Rev. A* **24**, 1643 (1981); **31**, 1788 (1985).
- [33] A. Onuki, *Phys. Rev. E* **55**, 403 (1997).
- [34] R. Folk and G. Moser, *Phys. Rev. E* **57**, 683 (1998); **57**, 705 (1998).
- [35] For the Cu wall used in Ref. [20], the longitudinal sound velocity is  $c_w = 5.0 \times 10^5 \text{ cm/s}$  and the mass density is  $\rho_w = 8.96 \text{ g/cm}^3$ . The acoustic impedance of the wall  $\rho_w c_w$  is three orders of magnitude larger than that of the fluid, so the transmission of sounds into the wall is negligible.
- [36] P. Carlès and B. Zappoli, *Phys. Fluids* **7**, 2905 (1995).
- [37] P. C. Hohenberg and M. Barmartz, *Phys. Rev. A* **6**, 289 (1972).
- [38] On reflection, the excess mass in the form of the localized mode at time  $t$  is given by the inverse Fourier transformation of  $a/\kappa = \alpha(1-Z)/ik$ . For  $t > t_0 > t'_B$ , it behaves as  $\Delta M(4t_2/\pi t)^{1/2}$  in accord with Eq. (3.49).
- [39] Yu. R. Chashkin, A. V. Voronel, V. A. Smirnov, and V. G. Gobunova, *Sov. Phys. JETP* **25**, 79 (1979).
- [40] A. Onuki, *Prog. Theor. Phys.* **99**, 382 (1990).
- [41] D. Dahl and M. R. Moldover, *Phys. Rev. A* **6**, 1915 (1972); G. R. Brown and H. Meyer, *ibid.* **6**, 364 (1972).
- [42] A. Onuki, *Phys. Rev. E* **75**, 036304 (2007).
- [43] J. Hegseth, A. Oprisan, Y. Garrabos, V. S. Nikolayev, C. Lecoutre-Chabot, and D. Beysens, *Phys. Rev. E* **72**, 031602 (2005).
- [44] R. Wunenburger, Y. Garrabos, C. Lecoutre, D. Beysens, J. Hegseth, F. Zhong, and M. Barmartz, *Int. J. Thermophys.* **23**, 103 (2002).